2 Millimeter Ultra Deep Field Observations

Johannes Staguhn

Observational Cosmology Laboratory, NASA Goddard Space Flight Center
& The Johns Hopkins University

GISMO Team

Dominic Benford[1], Eli Dwek[1], Dale Fixsen [1], Christine Jhabvala[1], Alexander Karim[4], Attila Kovacs[2], Samuel Leclercq[3], Stephen Maher[1], Tim Miller[1], S. Harvey Moseley[1], Eva Schinnerer[4], Elmer Sharp,[1] Fabian Walter[4], Edward Wollack[1]

[1]NASA's GSFC, [2]University of Minnesota, [3]IRAM, Grenoble, France, [4]MPIA Heidelberg, Germany

Motivation: Field Large Format Array Technologies: Backshort Under Grid (BUG)

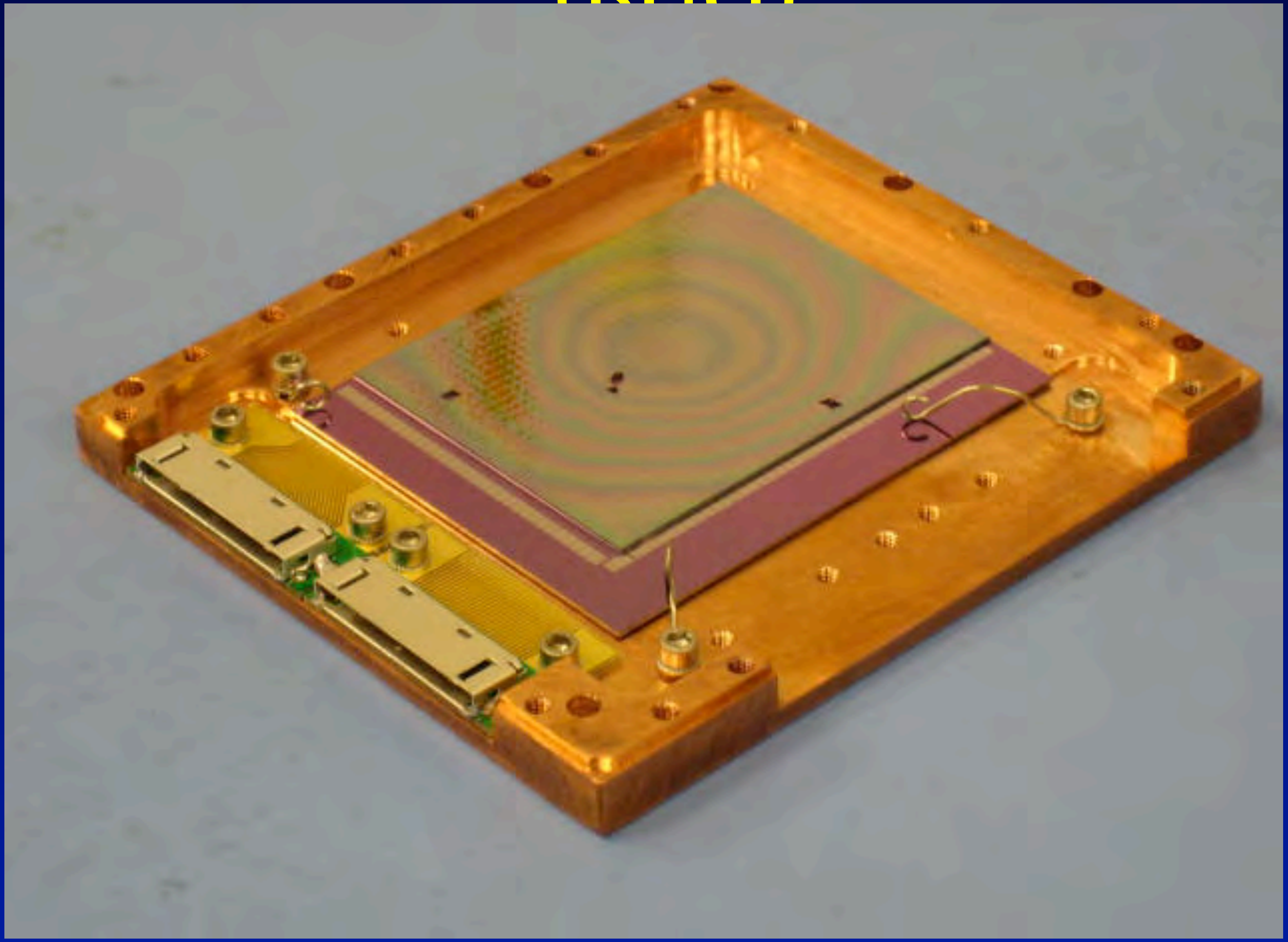

TES – Superconducting Bolometer

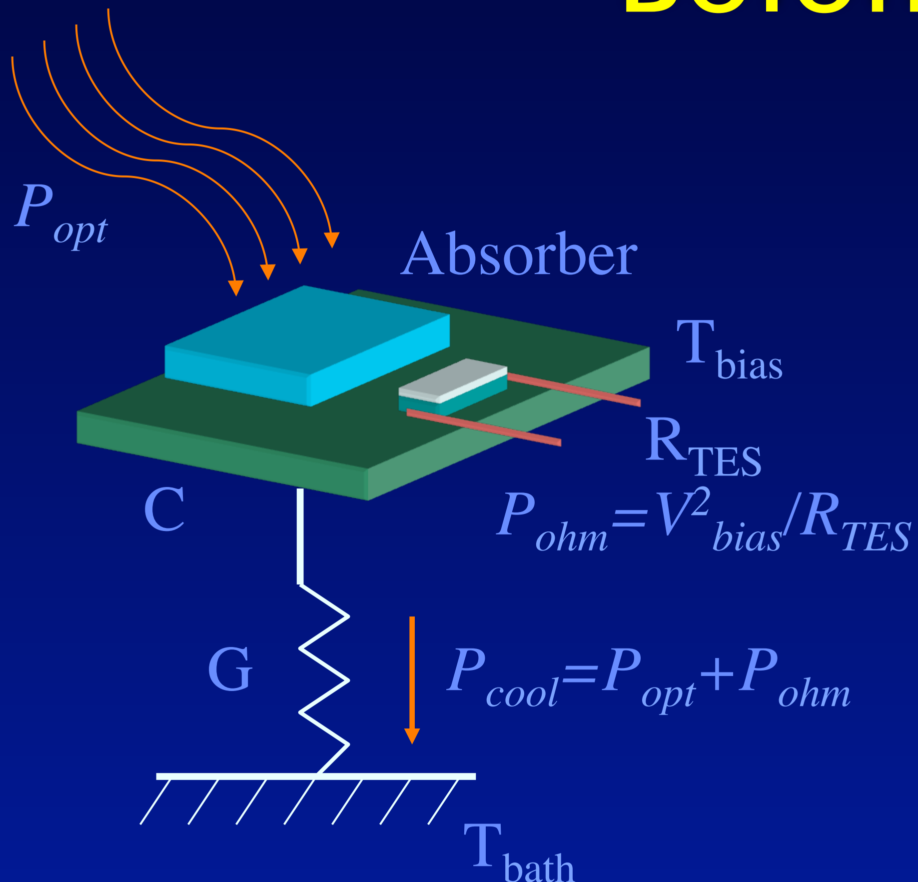

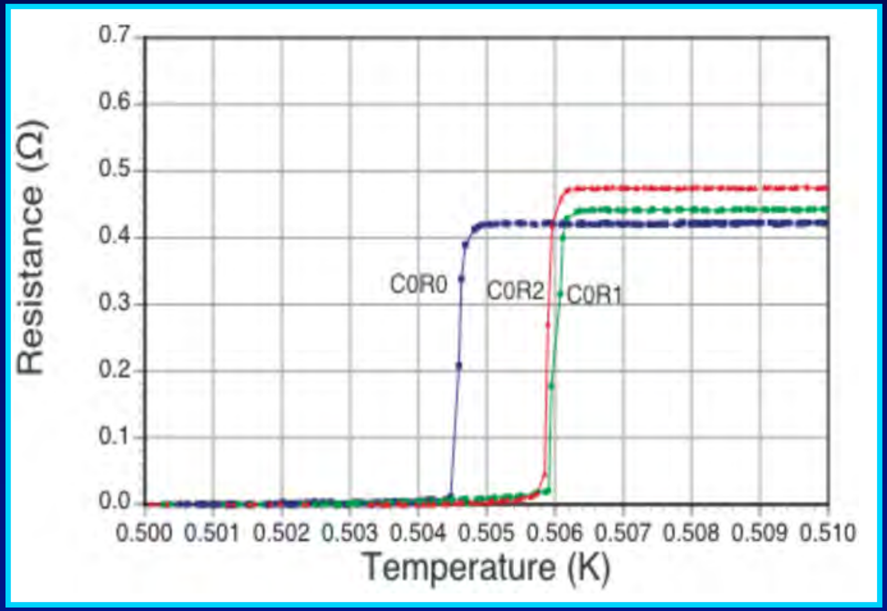

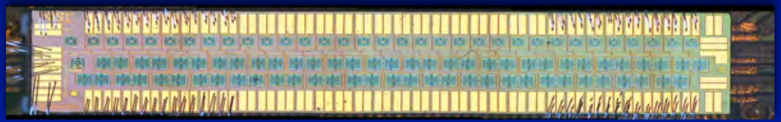

NIST SQUID Mux

Goddard-IRAM Superconducting 2-Millimeter Observer (GISMO)

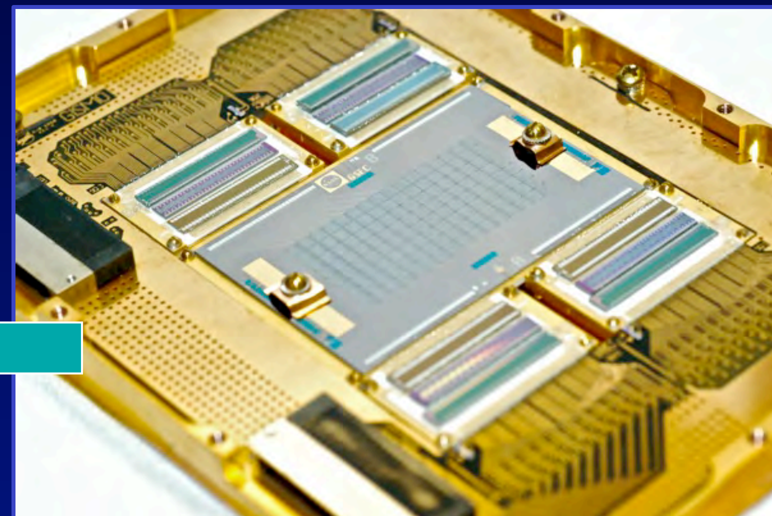

Backshort under Grid (BUG) TES detector array

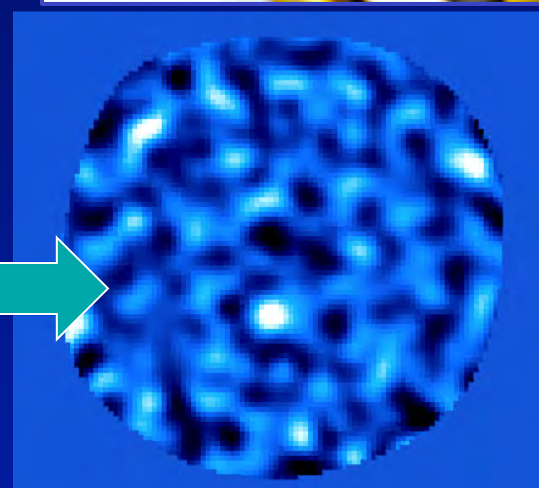

GISMO Deep Field (GDF)

GISMO 2mm Camera Science

Scientific Potential of a 2 mm Bolometer Camera

SED of Starburst Galaxy Arp 220 for different redshifts
GISMO 2000 μm

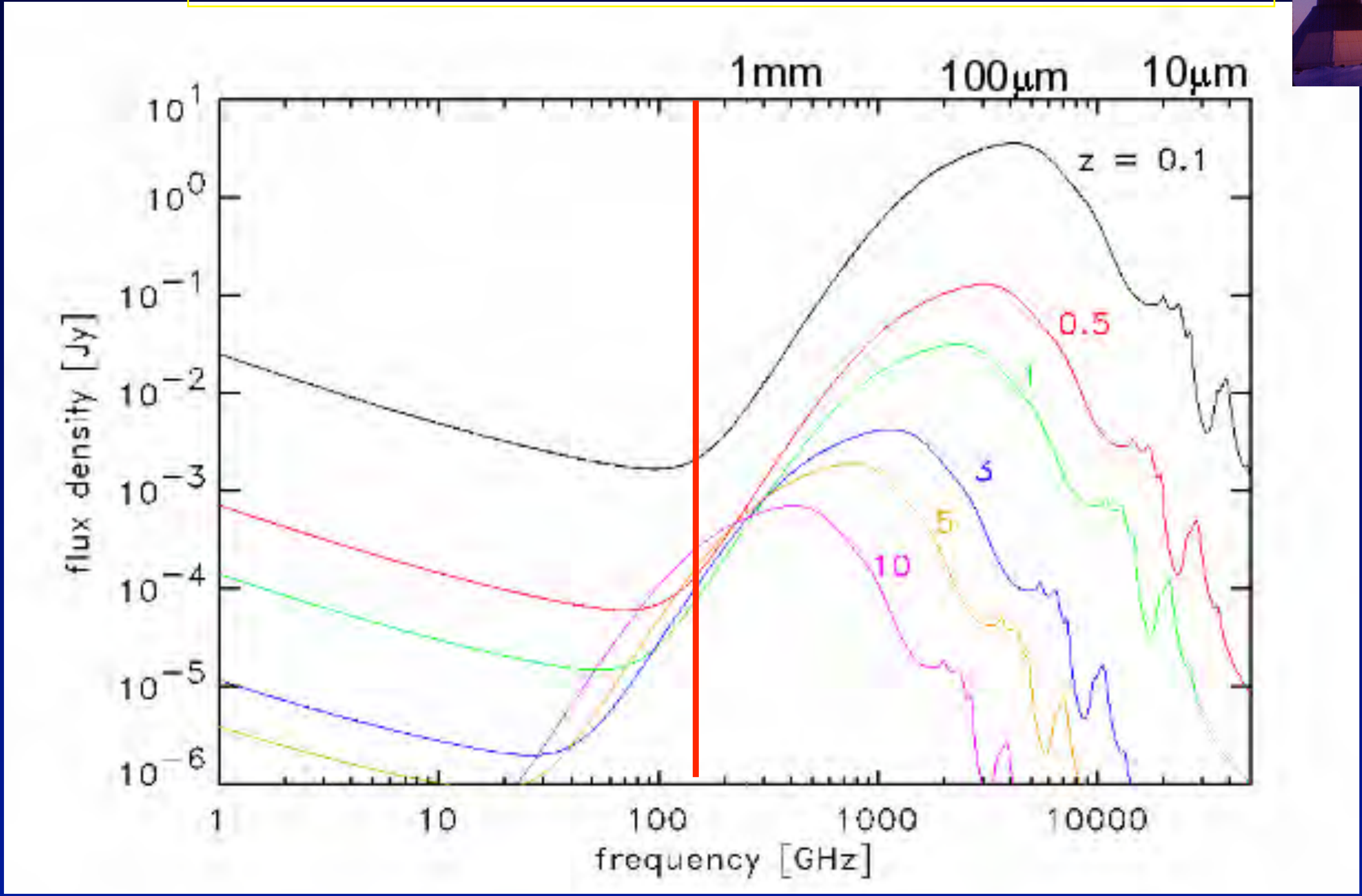

SED of Starburst Galaxy Arp 220 for different redshifts

Herschel 250, 350, 500 μm

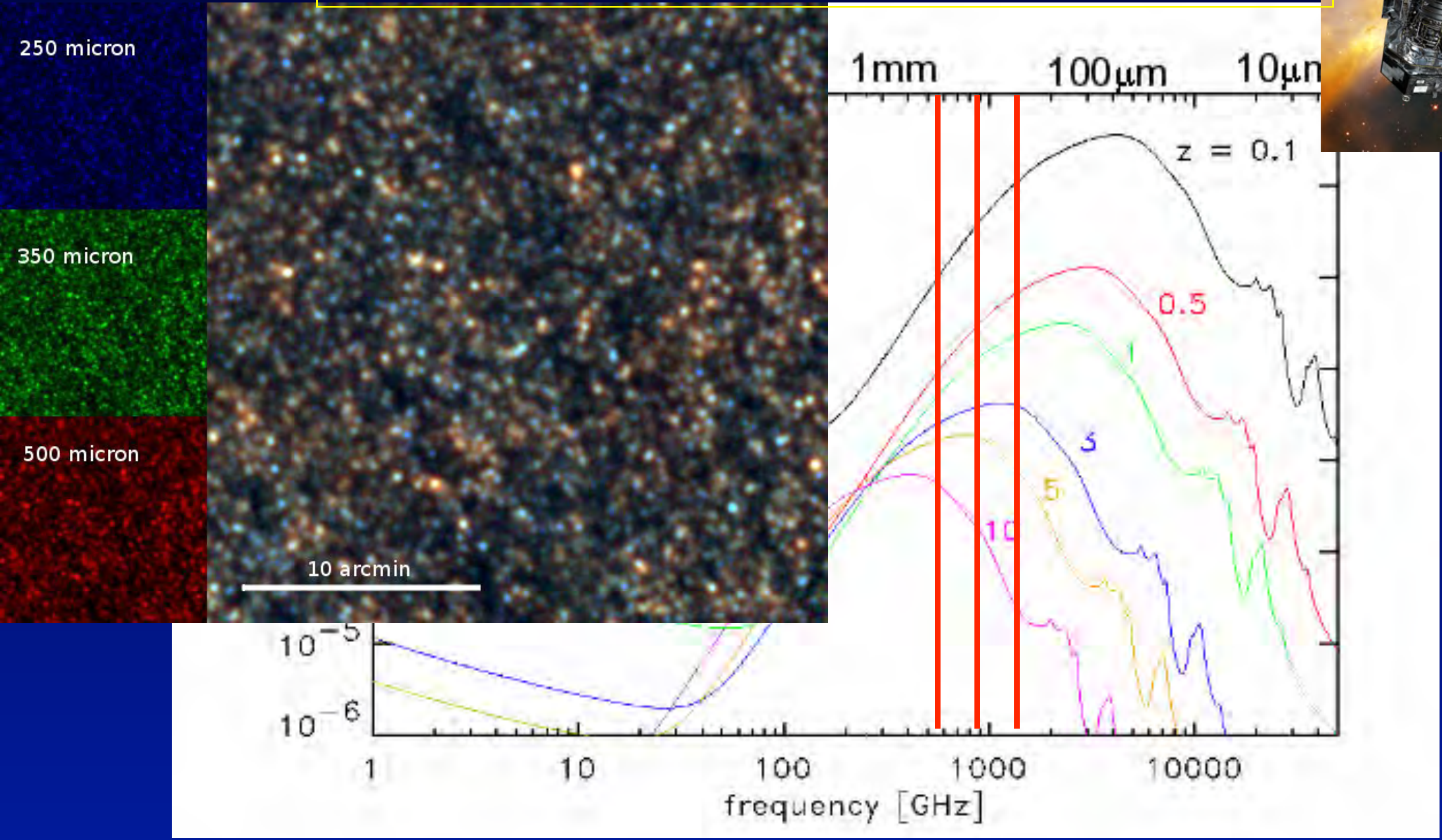

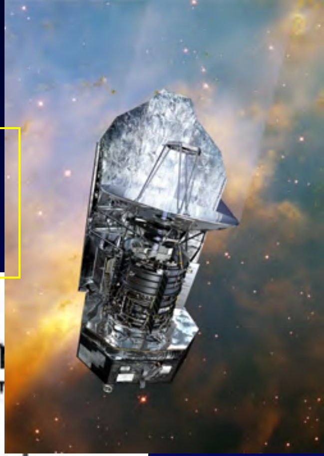

GISMO 2mm Camera Science

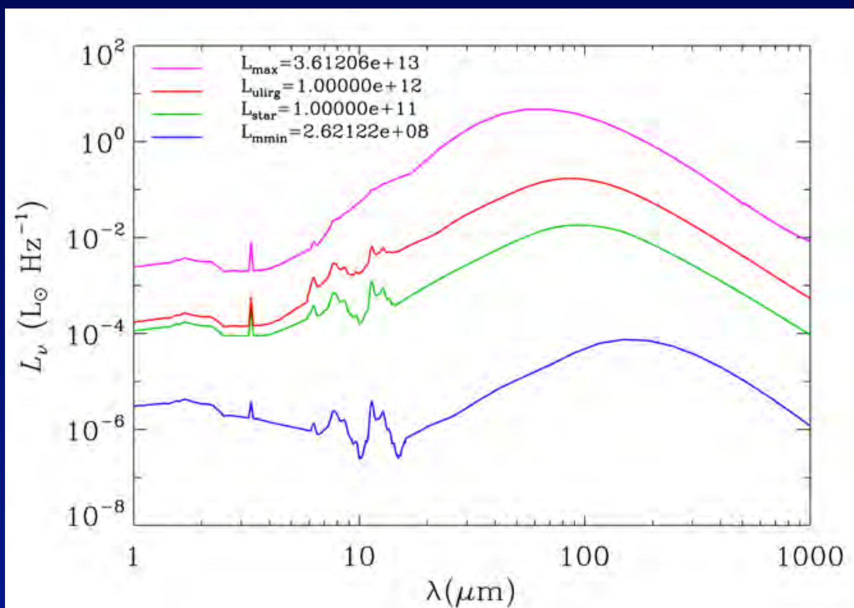

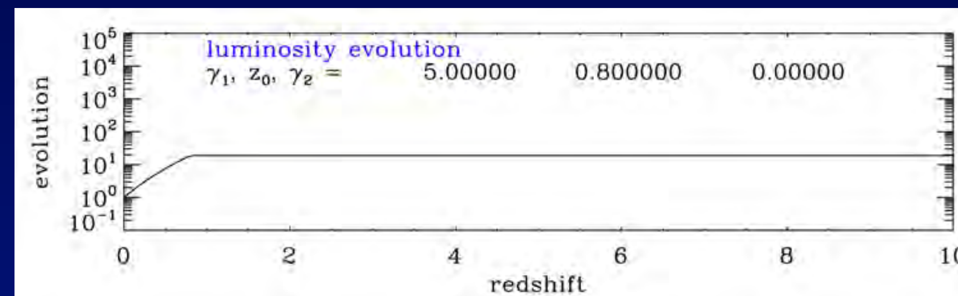

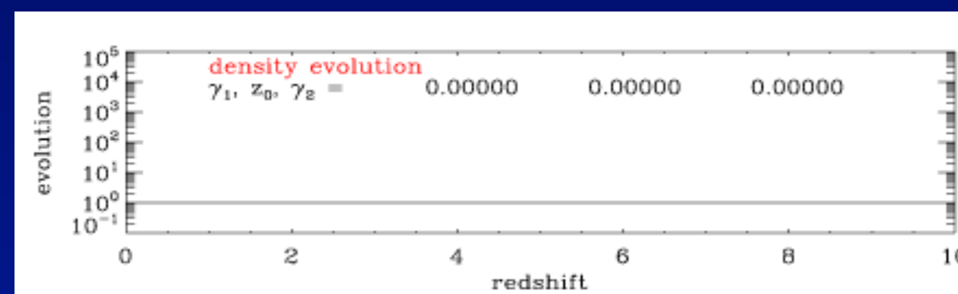

Template galaxy SEDs from Chary & Elbaz, 2001

GISMO 2mm Camera Science

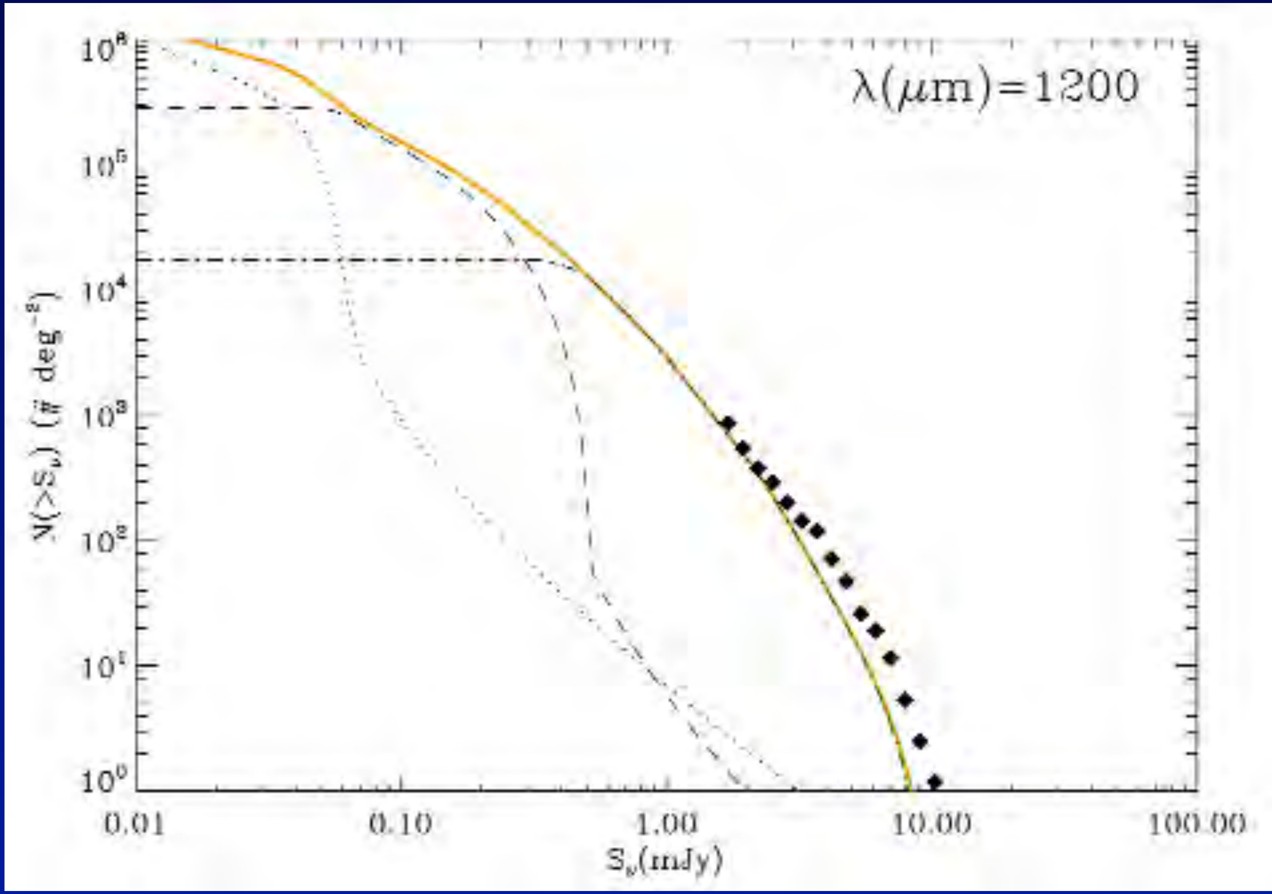

GISMO 2mm Camera Science

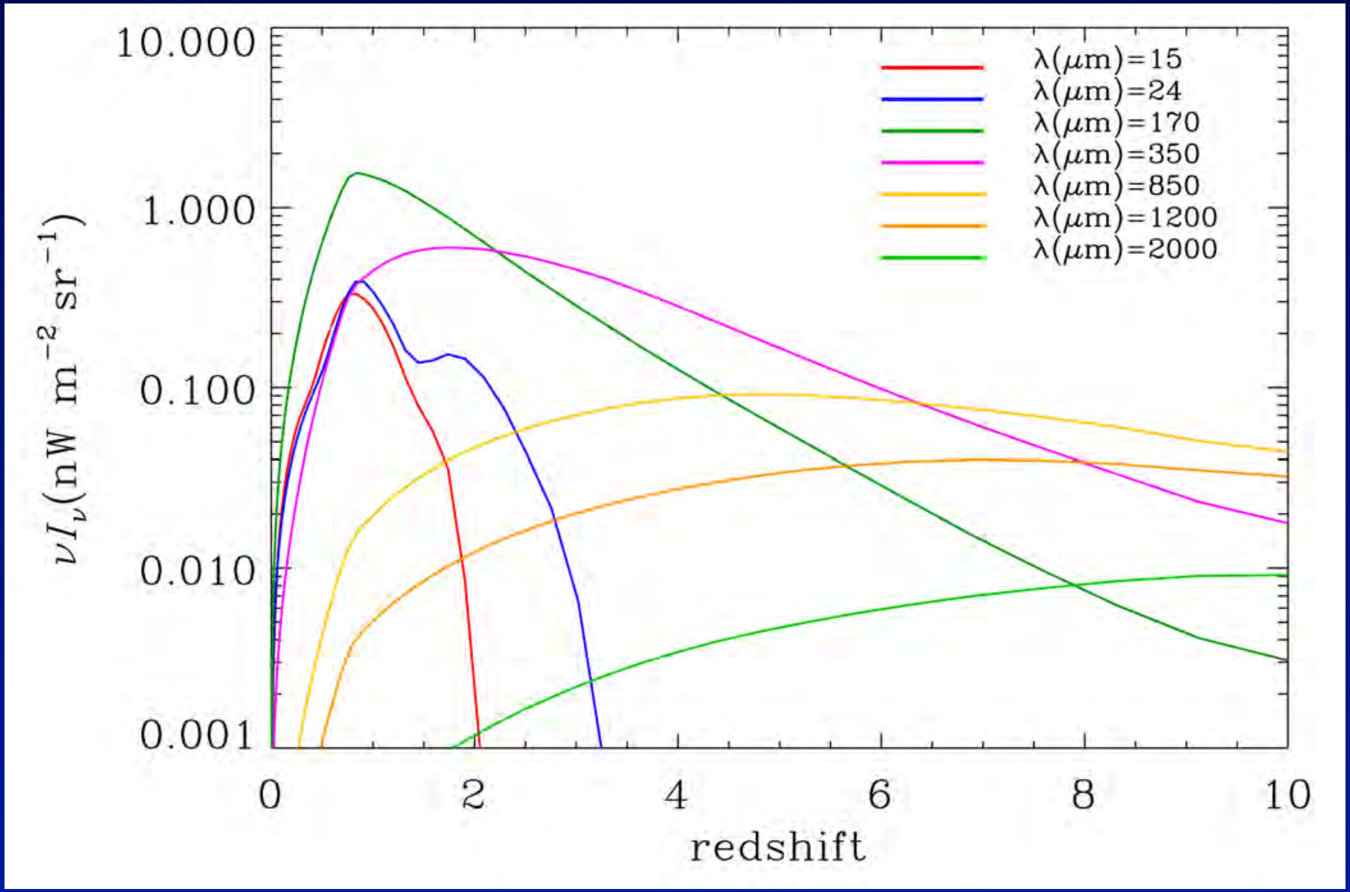

Beating the Confusion Limit

30 m Telescope:

: 1.2 mm

: 2 mm

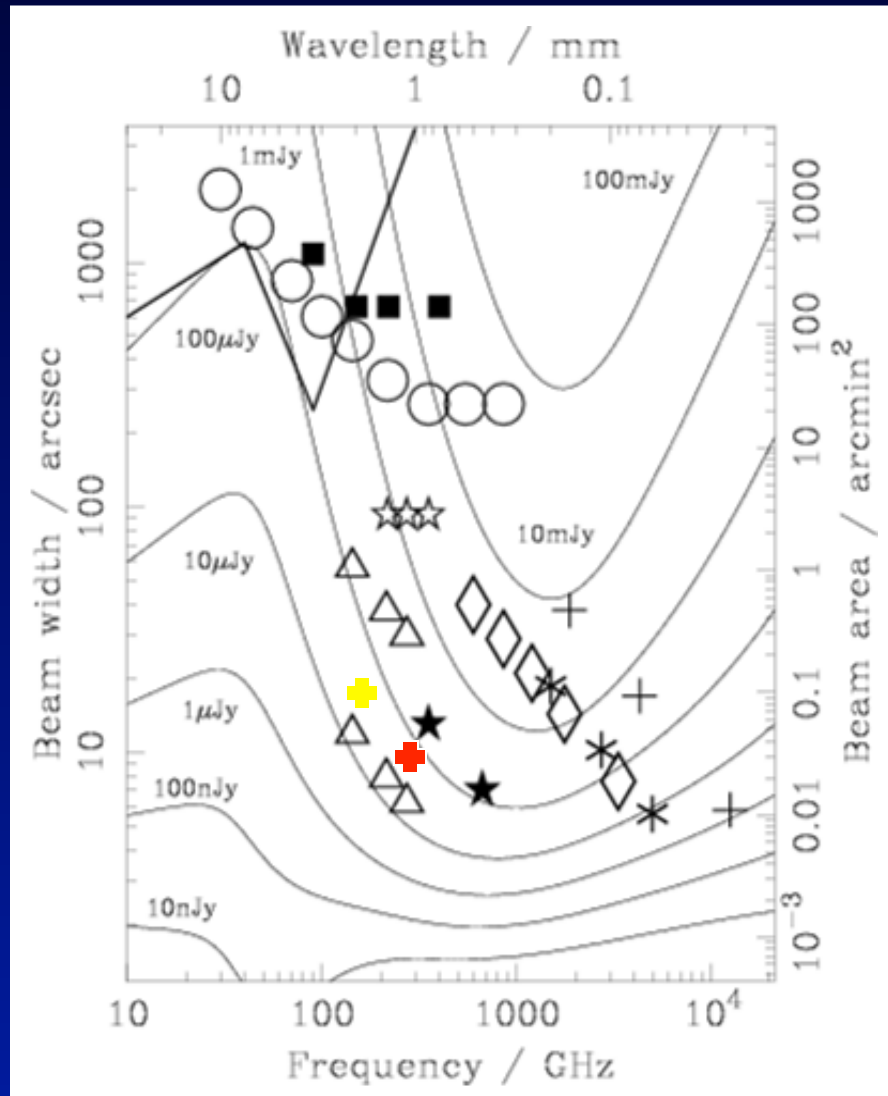

Plot: A. Blain

GISMO Source Count Modeling

GOODS-N data: ACS & NICMOS
traces galaxies up to z ~ 4

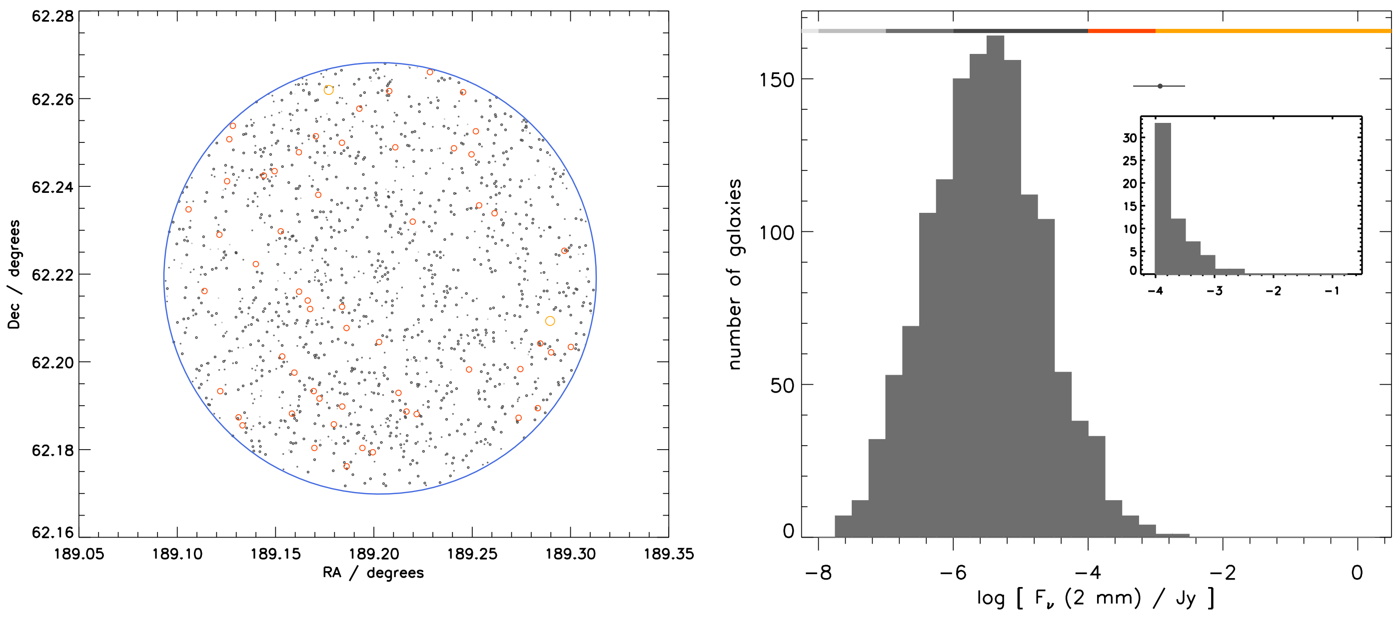

In collaboration with F. Walter & E. de Cunha

GISMO Camera


GISMO Performance

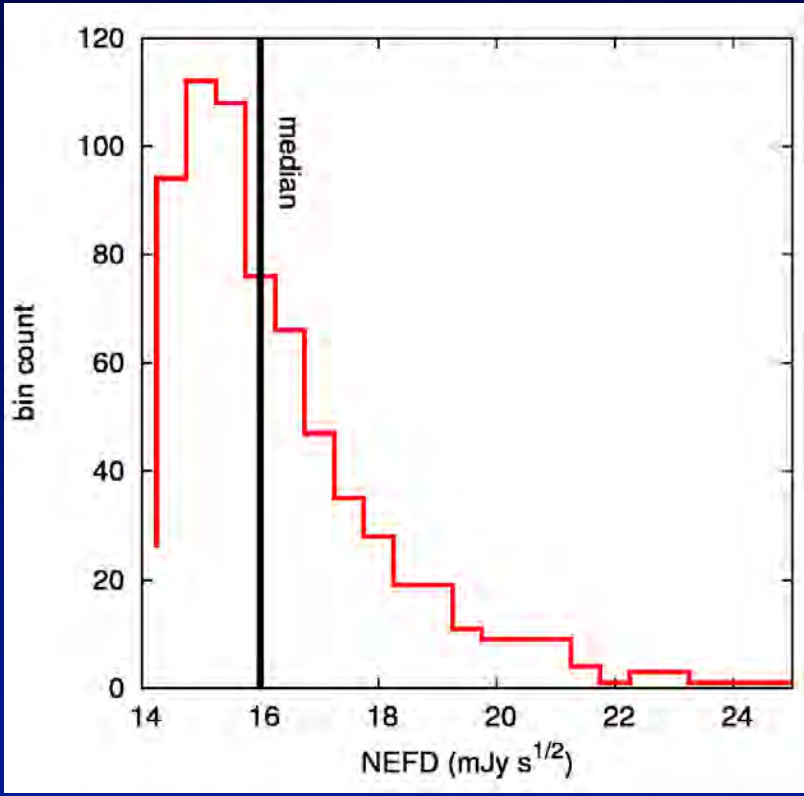

GISMO NEFD

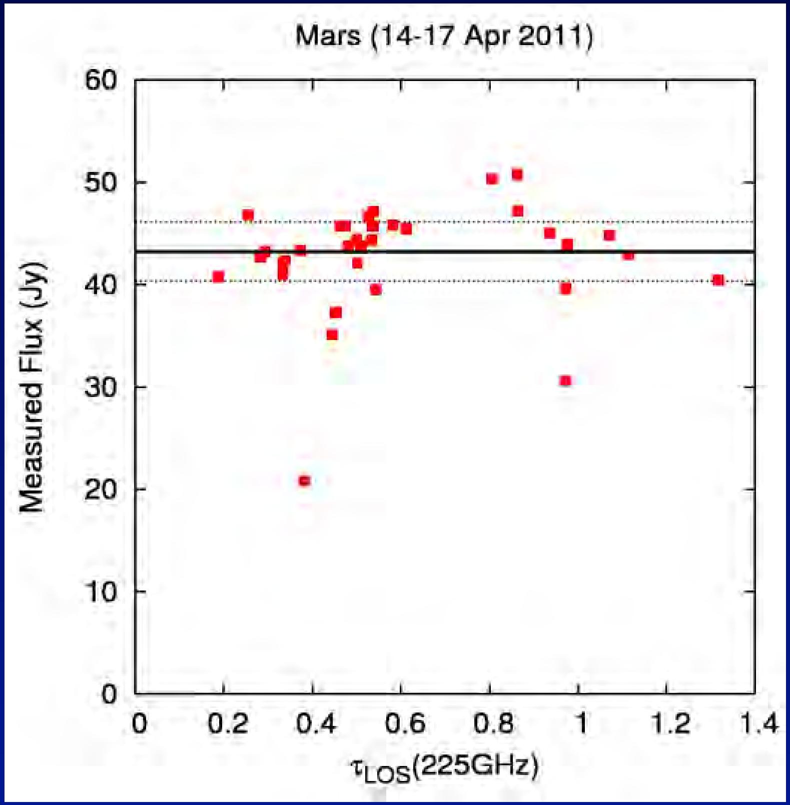

blind flux calibration rms: 7%
(note the range of of sky opacities)

GISMO Deep Field

rms in D~5' (shown): 130 μJy -190 μJy (so far deepest fields: SCUBA, AzTEC: ~ 400 μJy)

Entire ~ 7' x 7' field t_{int} = 25 hrs

calibration uncertainty: 7%

Herschel, SCUBA, MAMBO-2 Counterpart

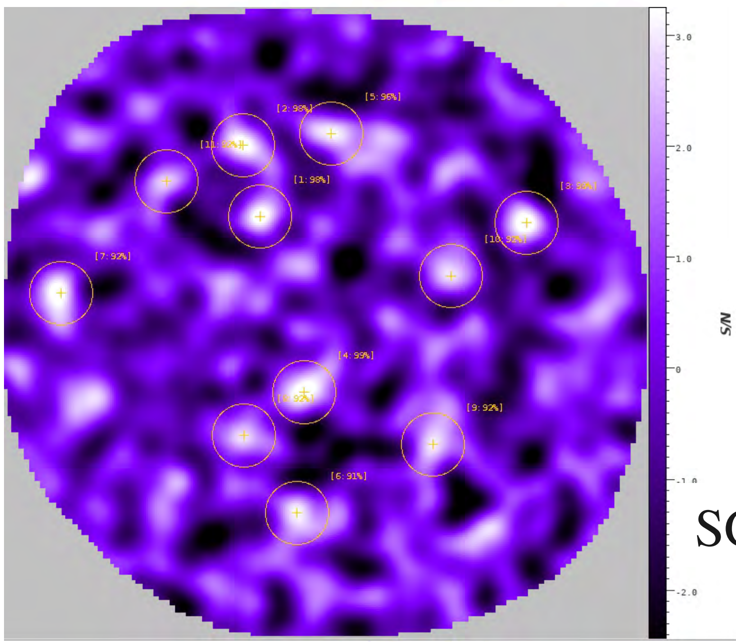

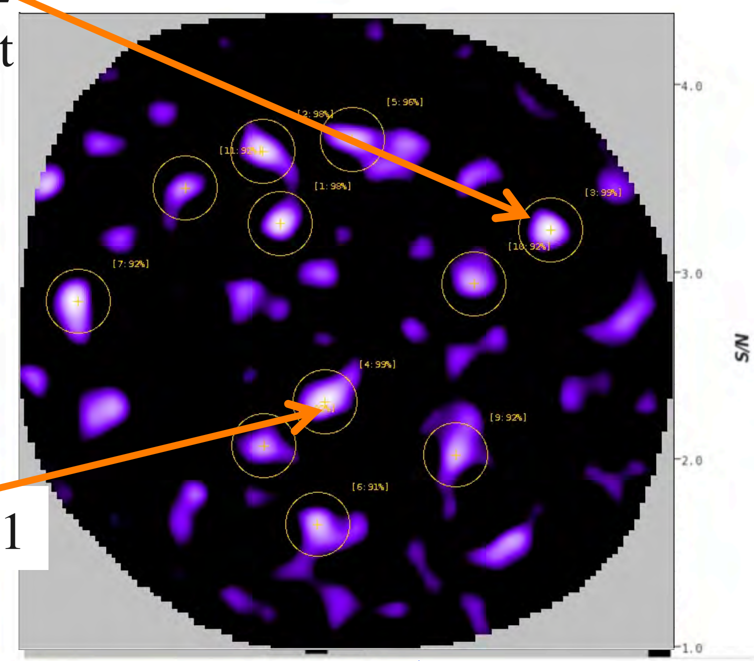

SCUBA 850.1

measured flux of detected sources between ~400 μJy and 700 μJy

GISMO 2mm Camera Science

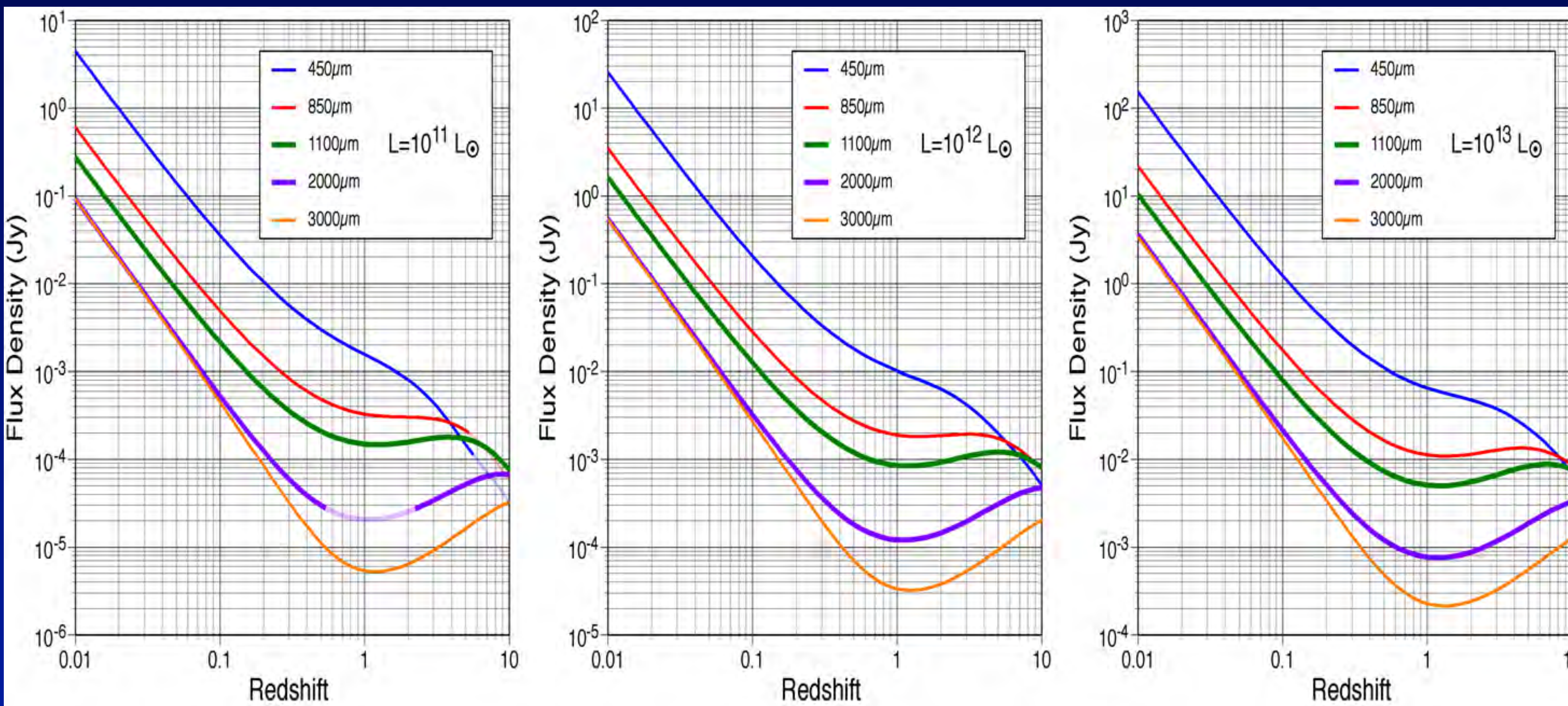

GISMO Deep Field Noise Histogram

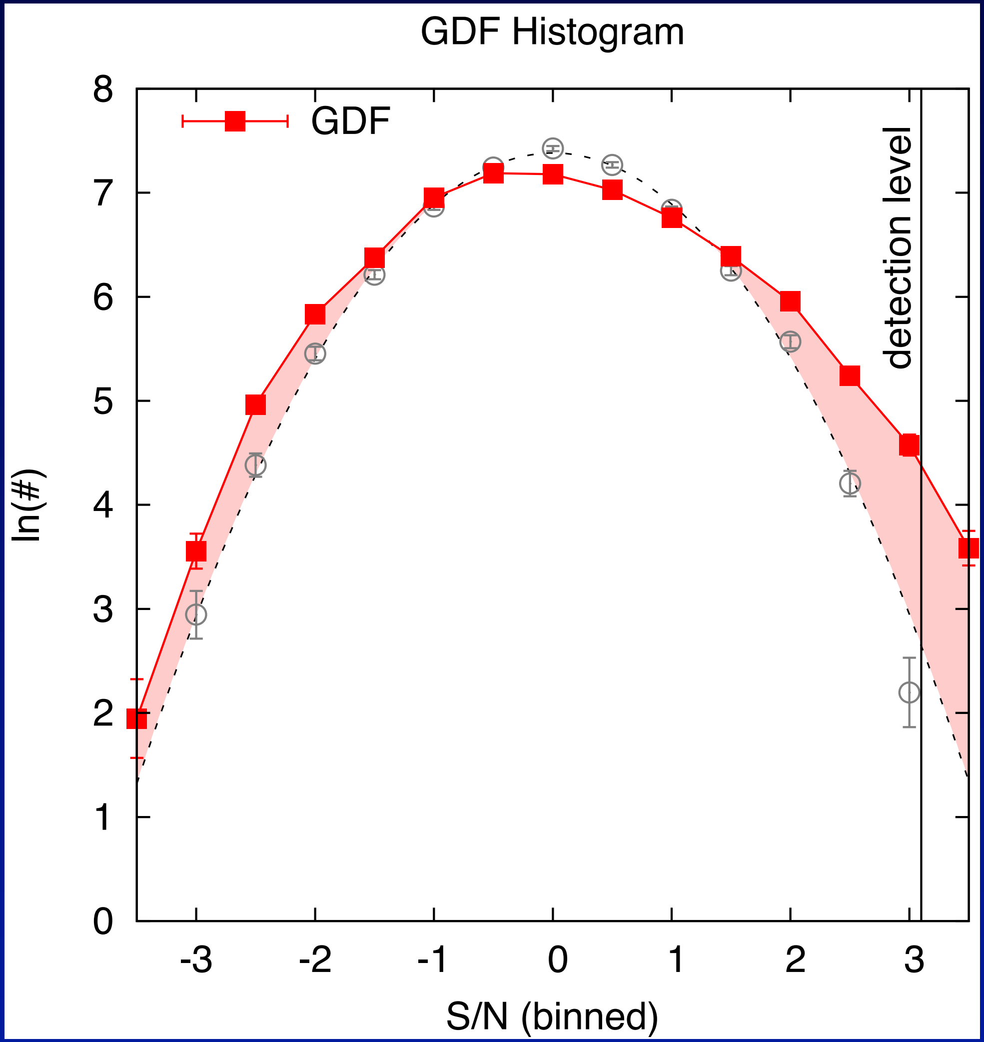

Grey symbols:
Jackknifed GDF data

Dahed grey line:
Gaussian distribution

Red Symbols:
GDF Data

Stacking Analysis

THE DATASET:
The GOODS-N field

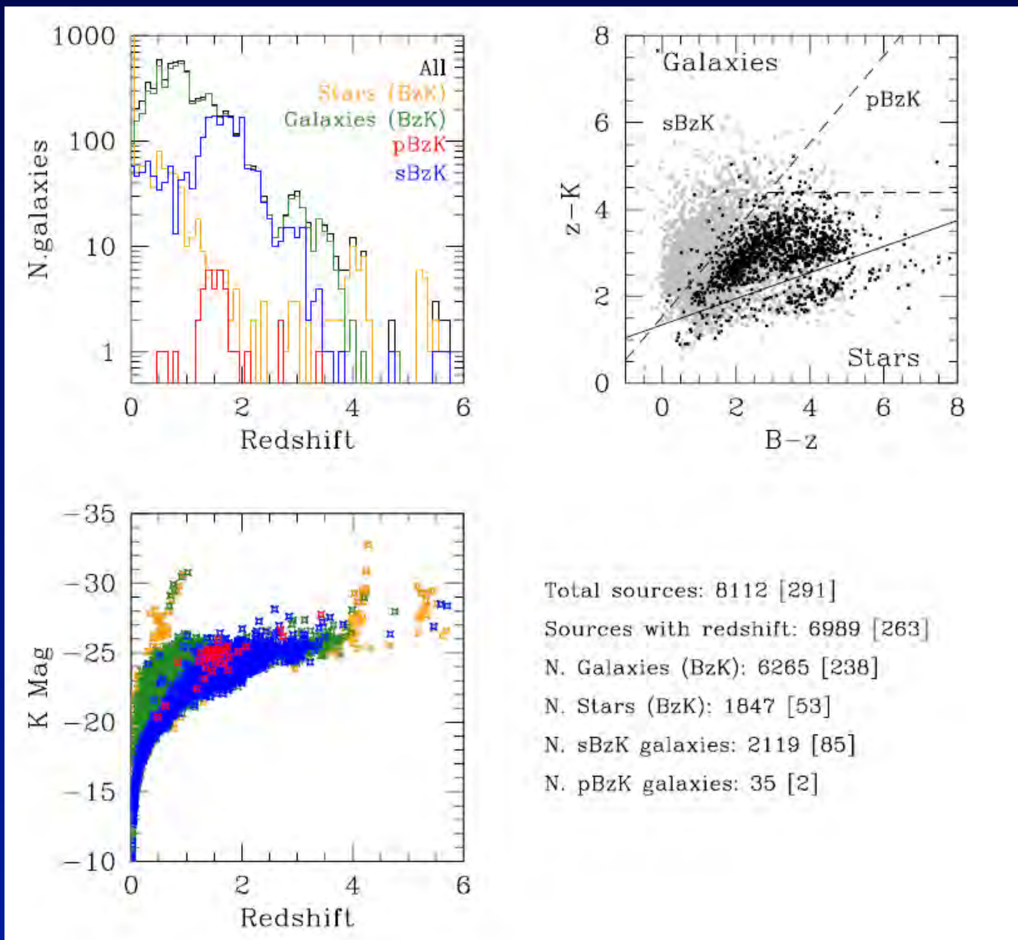

8112 galaxies with *bvizK* fluxes from Bundy et al. (2009)

sBzK galaxies: star-forming galaxies selected so that (z-K) > (b-z) + 1.532

2119 sBzK galaxies in the catalogue

GISMO observations

0^{th} order analysis, extremely tentative!!!!

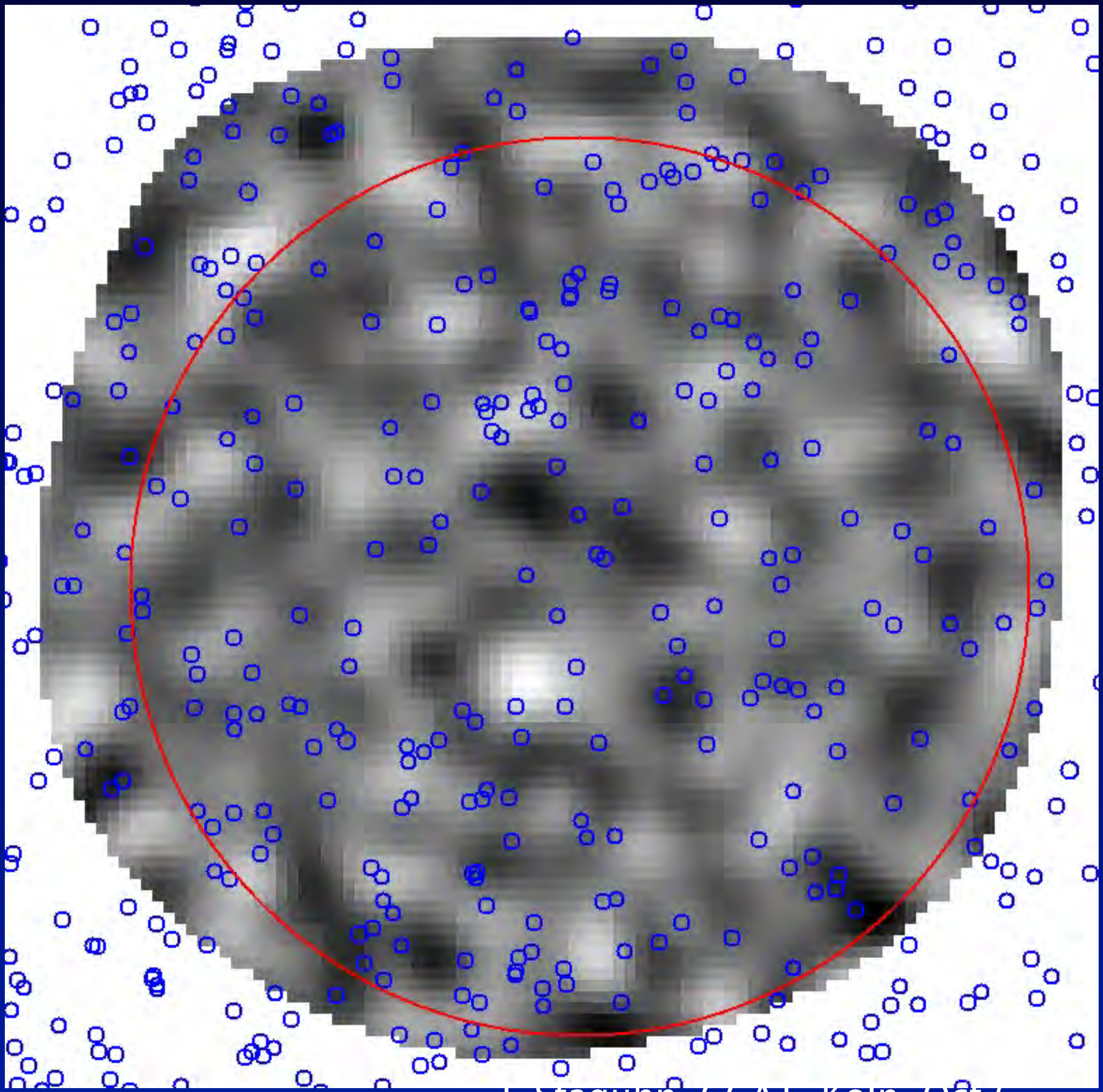

Grey scale: GISMO map of the HDF

sBzK galaxies are marked in blue

The red circle highlights the region used for the stacking analysis: 4' wide, including 212 sBzK galaxies

We correct for S/N variations using this sensitivity map:

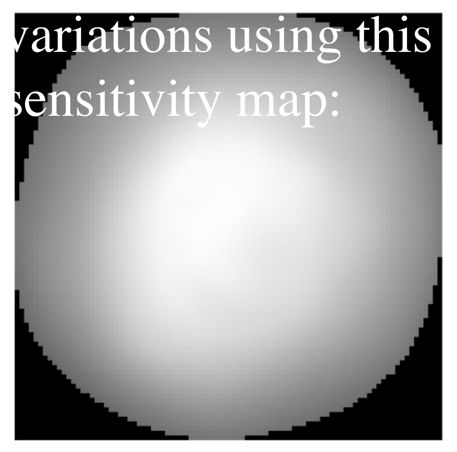

Stacking results from the GISMO observations

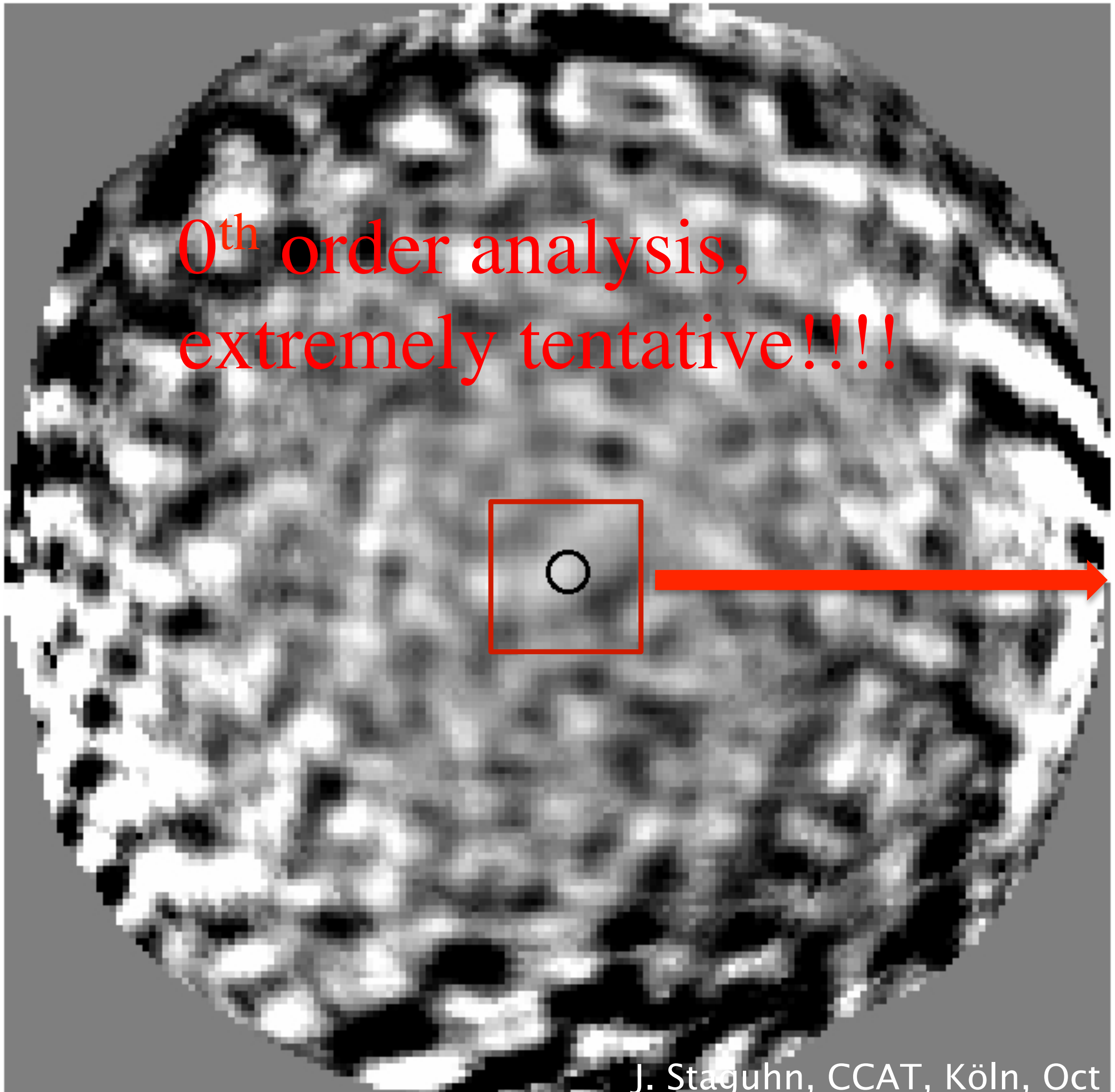

The stacking analysis gives an rms of ~15 – 20 uJy, and a tentative (~3sigma) detection at the map center.

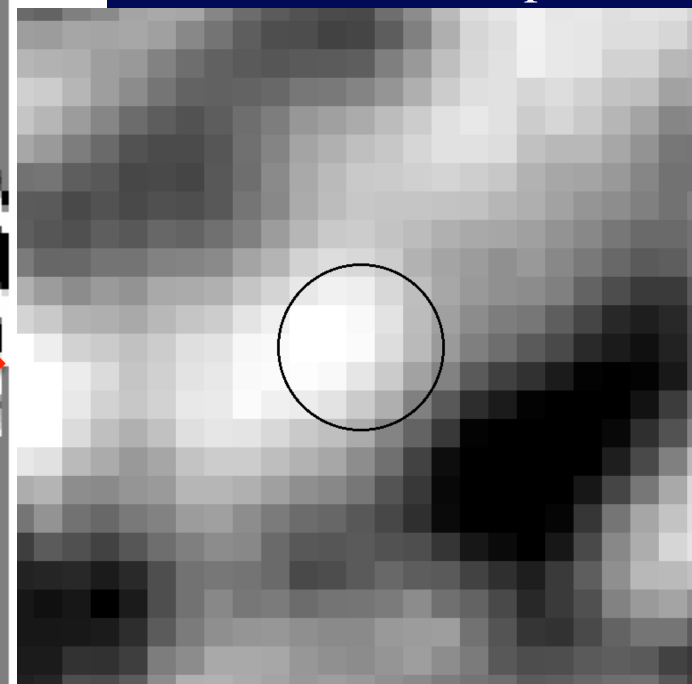

The circle marks the region corresponding to 1 primary beam

statistical analysis

0th order analysis, extremely tentative!!!!

We re-perform N-times the stacking over N-1 galaxies

This allows us to understand if there is any bright galaxy dominating the stacking results

This analysis shows that no individual source is contributing for more than 5% to the total stacked flux, i.e., the stacked flux is genuinely representative of the average population

J.

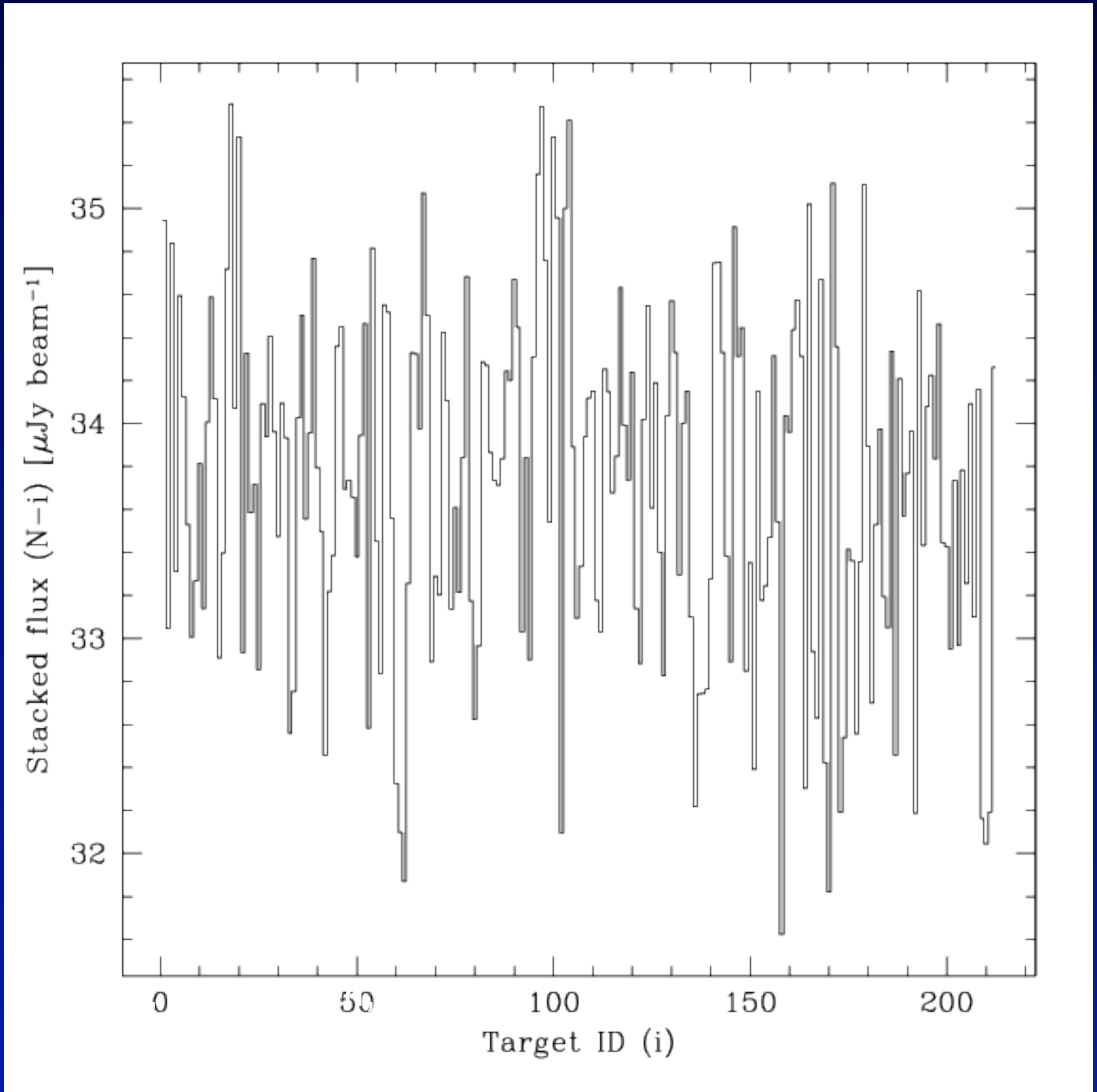

GISMO detection of z = 5.3 sub-mm galaxy AzTE

GISMO 2mm image of AzTEC-3

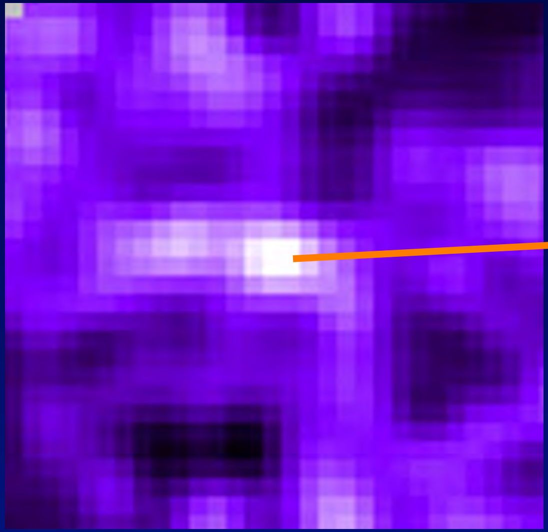

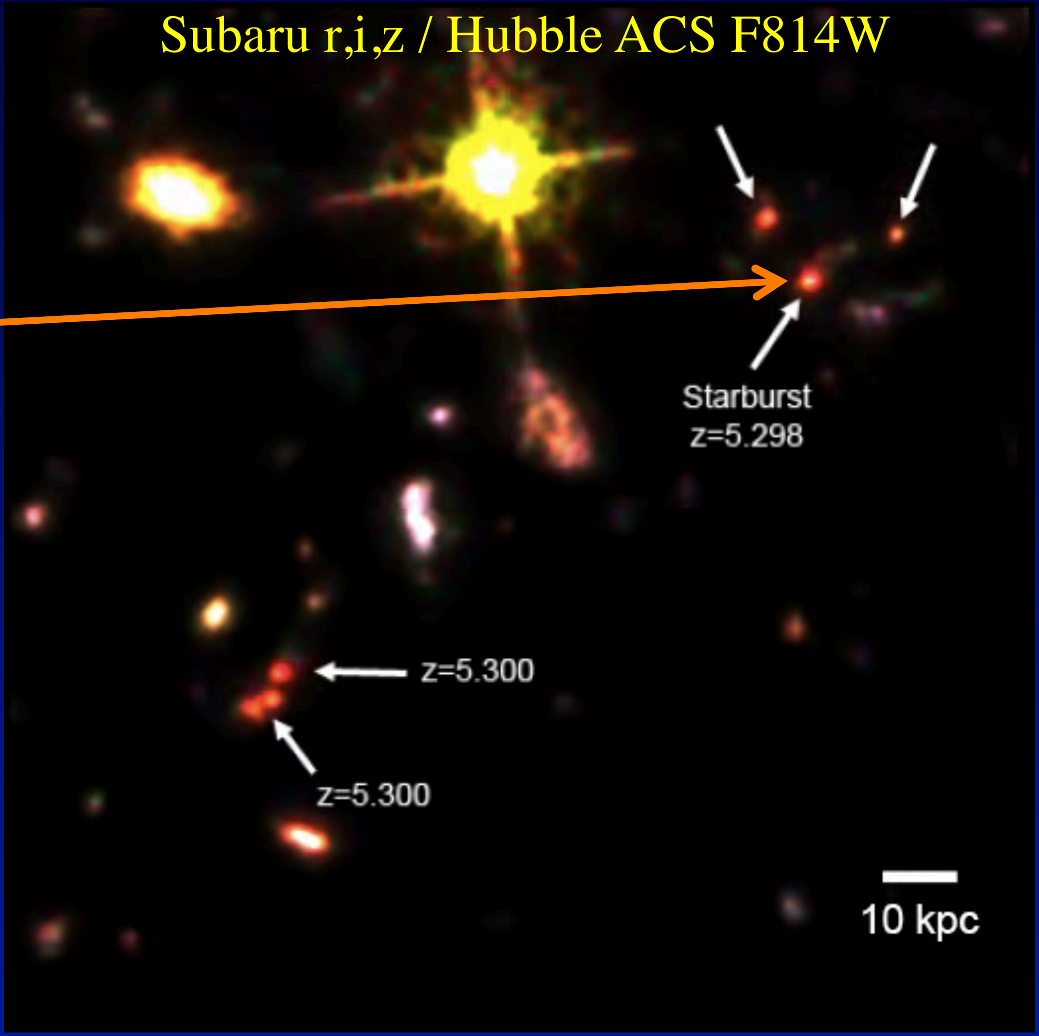

Extreme Star Formation In A Proto-Cluster During The First Billion Years Of Cosmic Time

Peter L. Capak[1], Dominik Riechers[2,3], Nick Z. Scoville[2], Chris Carilli[4], Pierre Cox[5], Roberto Neri[5], Brant Robertson[2,3], Mara Salvato[6], Eva Schinnerer[6], Lin Yan[1], Grant W. Wilson[7], Min Yun[7], Francesca Civano[8], Martin Elvis[8], Alexander Karim[6], Bahram Mobasher[9], & Johannes G. Staguhn[10]

Capak et al., 2011, Nature, 470, 233

Self-Consistent Solutions for Properties of AzTEC-3

Dwek et al., 2011, ApJ, 738, 36;

Self-consistent Solutions for Properties of AzTEC-3

Step 1: Determining the FIR luminosity and dust mass

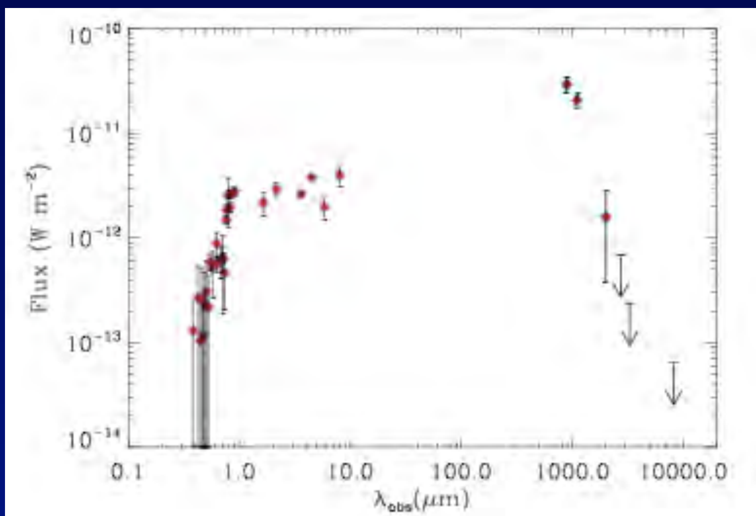

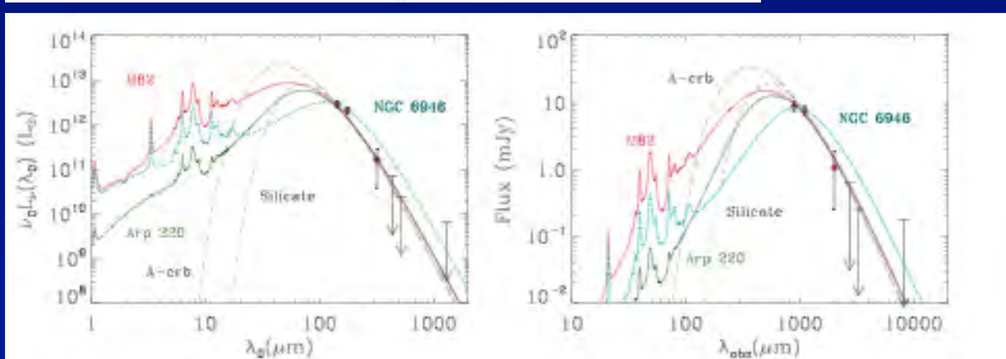

Table 2. Derived Temperatures, Masses, and IR Luminosities for Different Dust Compositions and Galaxy Templates

Composition	T_d (K)	M_d ($10^9 M_\odot$)	L_{IR} ($10^{13} L_\odot$)	κ (cm^2 g^{-1})[1]
Fe[2]	32.4± 6.1	$(1.4^{+1.2}_{-0.7})$	$(0.6^{+0.4}_{-0.2})$	16.5
Graphite	27.5±4.5	$(2.2^{+4.6}_{-2.2})$	$(0.5^{+0.3}_{-0.2})$	17.6
Silicate	28.5± 4.3	$(3.2^{+2.6}_{-1.4})$	$(0.6^{+0.4}_{-0.2})$	10.5
A-carbon	46.9±14.8	$(0.3^{+0.35}_{-0.17})$	$(1.1^{+1.7}_{-0.67})$	28.0
$\lambda^{-2} \times B_\nu$	29.3±4.8	$(0.6^{+0.6}_{-0.3})$	$(0.6^{+0.4}_{-0.2})$	50.0
Fe needles[3]	29.3±4.8	$(0.6^{+0.6}_{-0.3})$	$(0.6^{+0.4}_{-0.2})$	50.0
graphite needles[3]	29.3±4.8	$(0.6^{+0.6}_{-0.3})$	$(0.6^{+0.4}_{-0.2})$	···
M 82 template	···	(2.6 ± 0.9)	(1.7±0.6)	···
Arp 220 template	···	(1.4 ± 0.8)	(0.8±0.5)	···
NGC 6946 template	···	(18 ± 8)	(0.6±0.3)	···

[1]At wavelength $\lambda = 174.6\ \mu m$.

[2]Fe mass was calculated for a grain radius of 0.33 μm. See text for details.

[3]See text for details.

Self-consistent Solutions for Properties of AzTEC-3

Step 2: Converting L_{bol} to a Star Formation Rate

The conversion factor depends on:

(1) The stellar initial mass function (IMF):

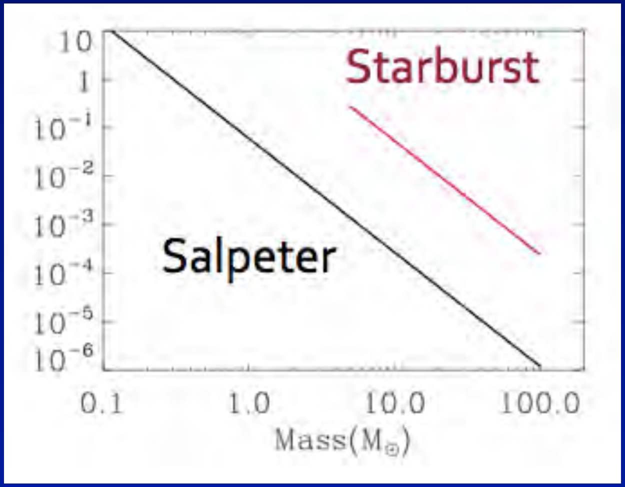

(2) The age of the starburst:

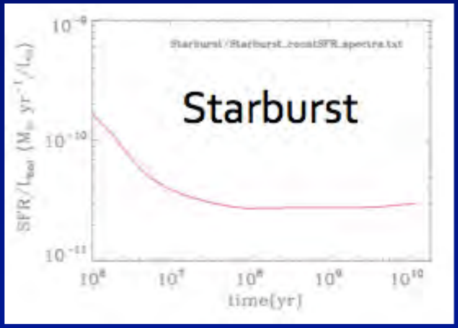

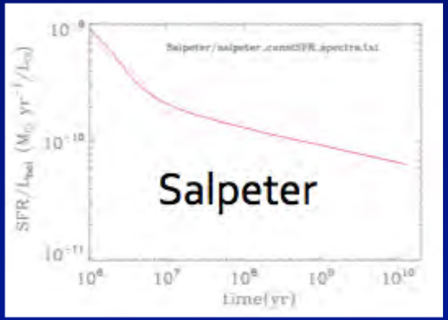

Self-consistent Solutions for Properties of AzTEC-3

Step 3: Fitting the Stellar SED

(PEGASE population synthesis code, Calzetti extinction law)

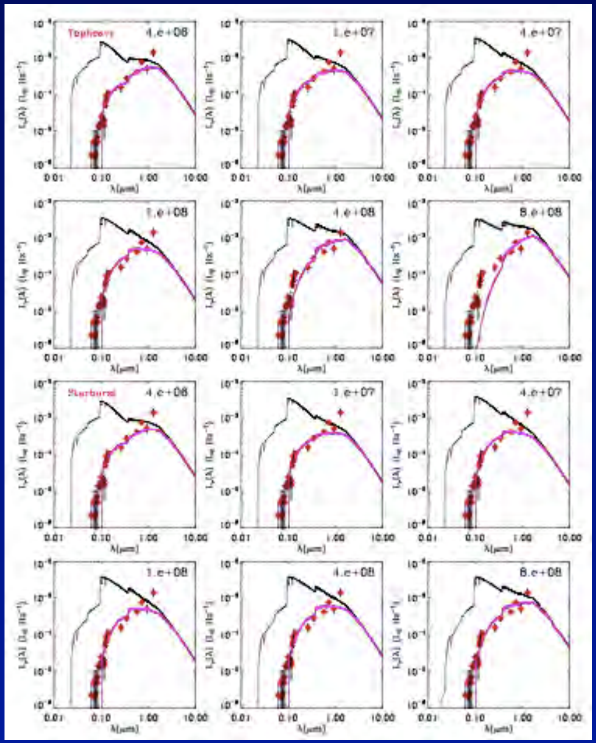

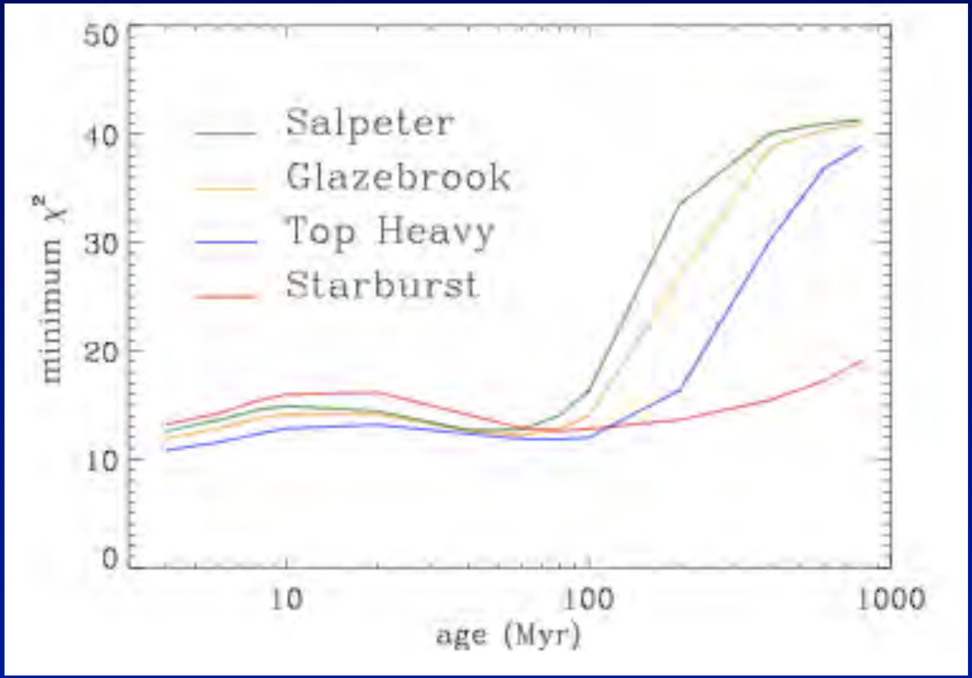

Self-consistent Solutions for Properties of AzTEC-3

Step 4a: apply observational constraints: stellar mass

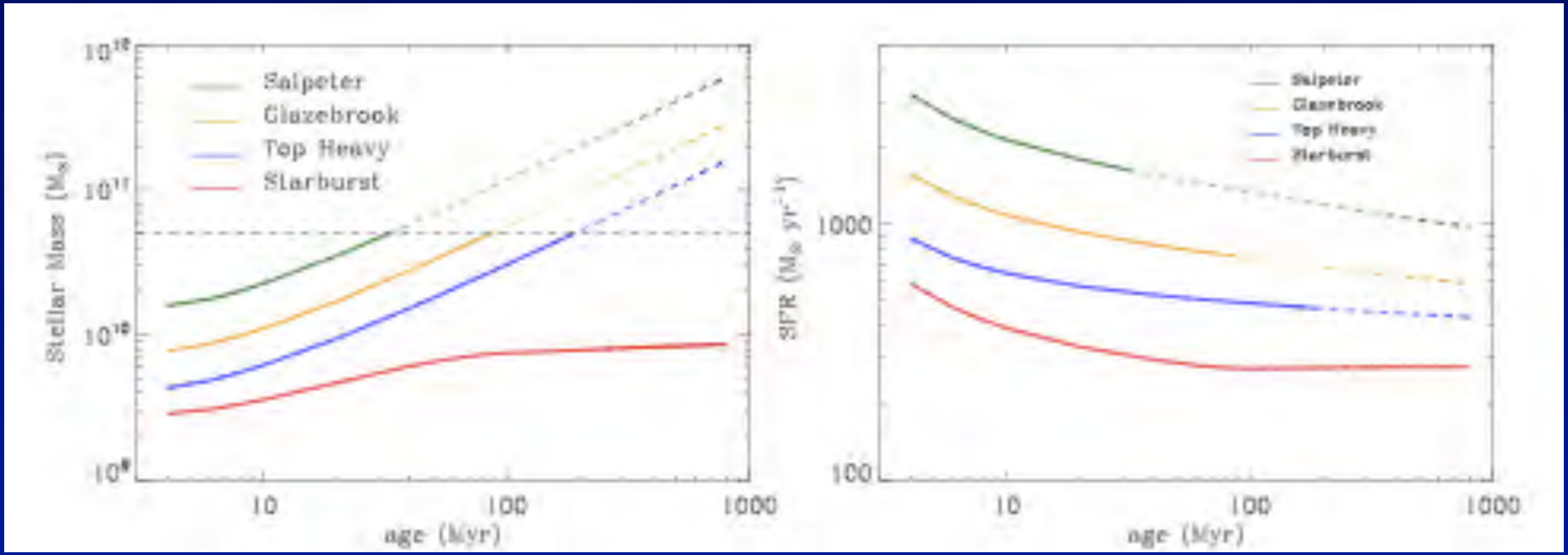

Self-consistent Solutions for Properties of AzTEC-3

Step 4b: apply observational constraints: dust mass

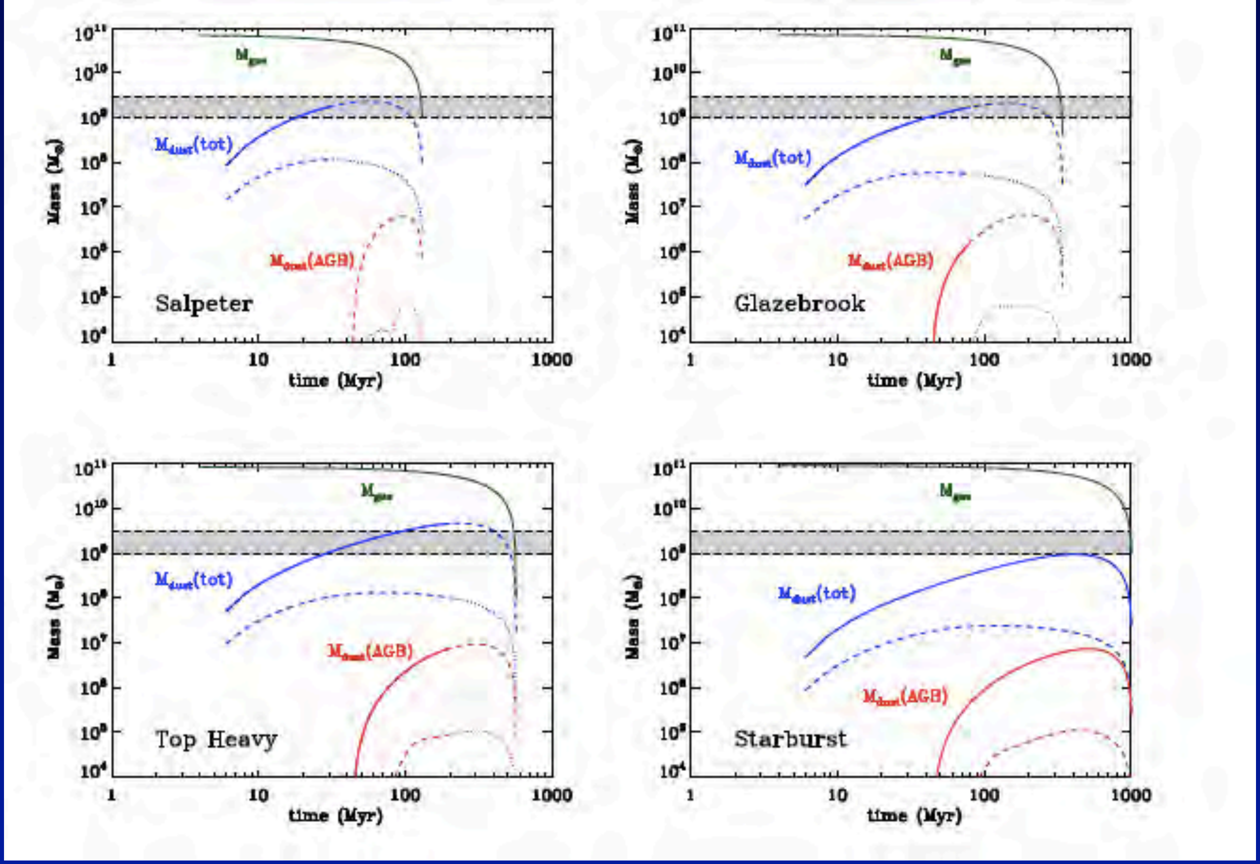

Self-consistent Solutions for Properties of AzTEC-3

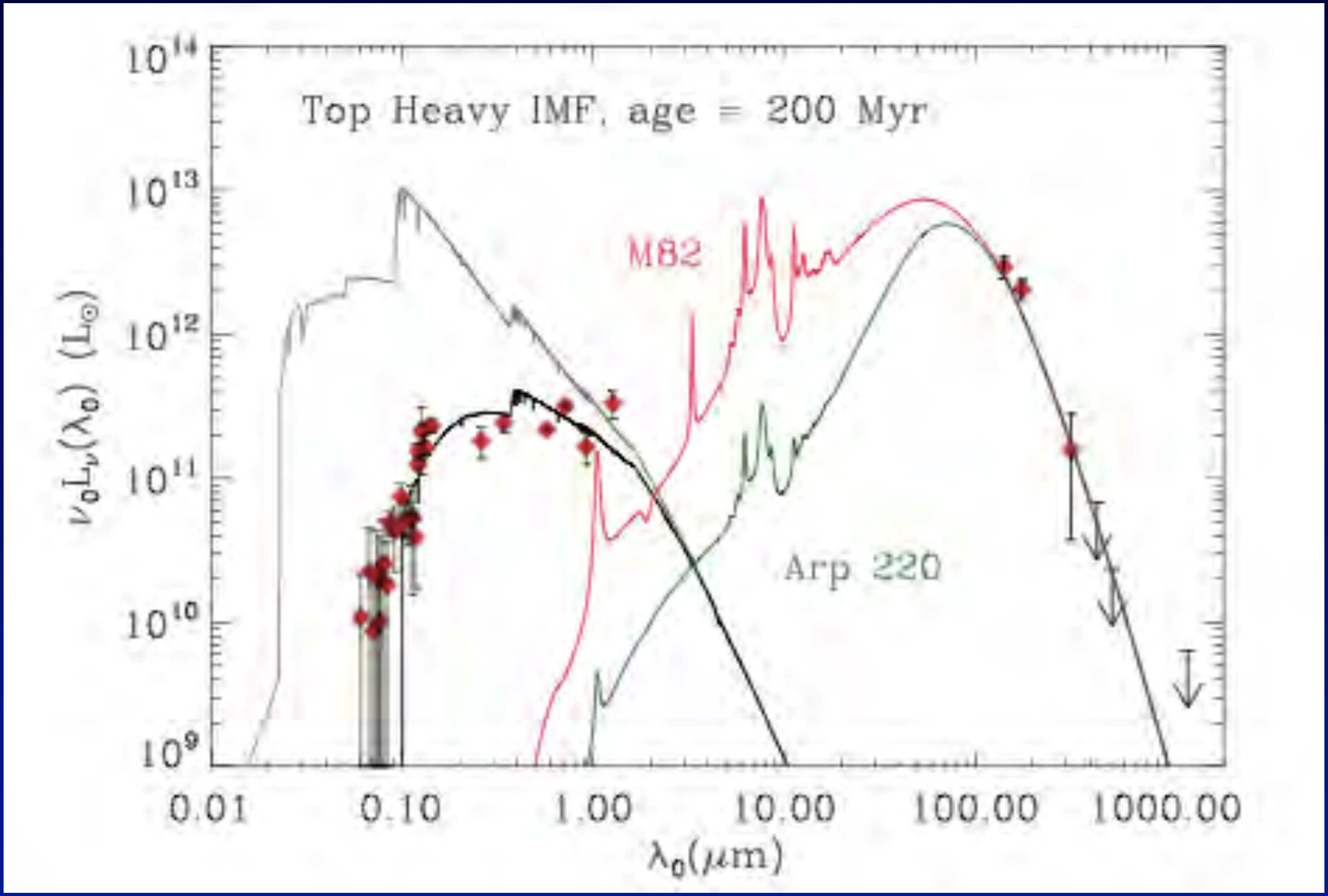

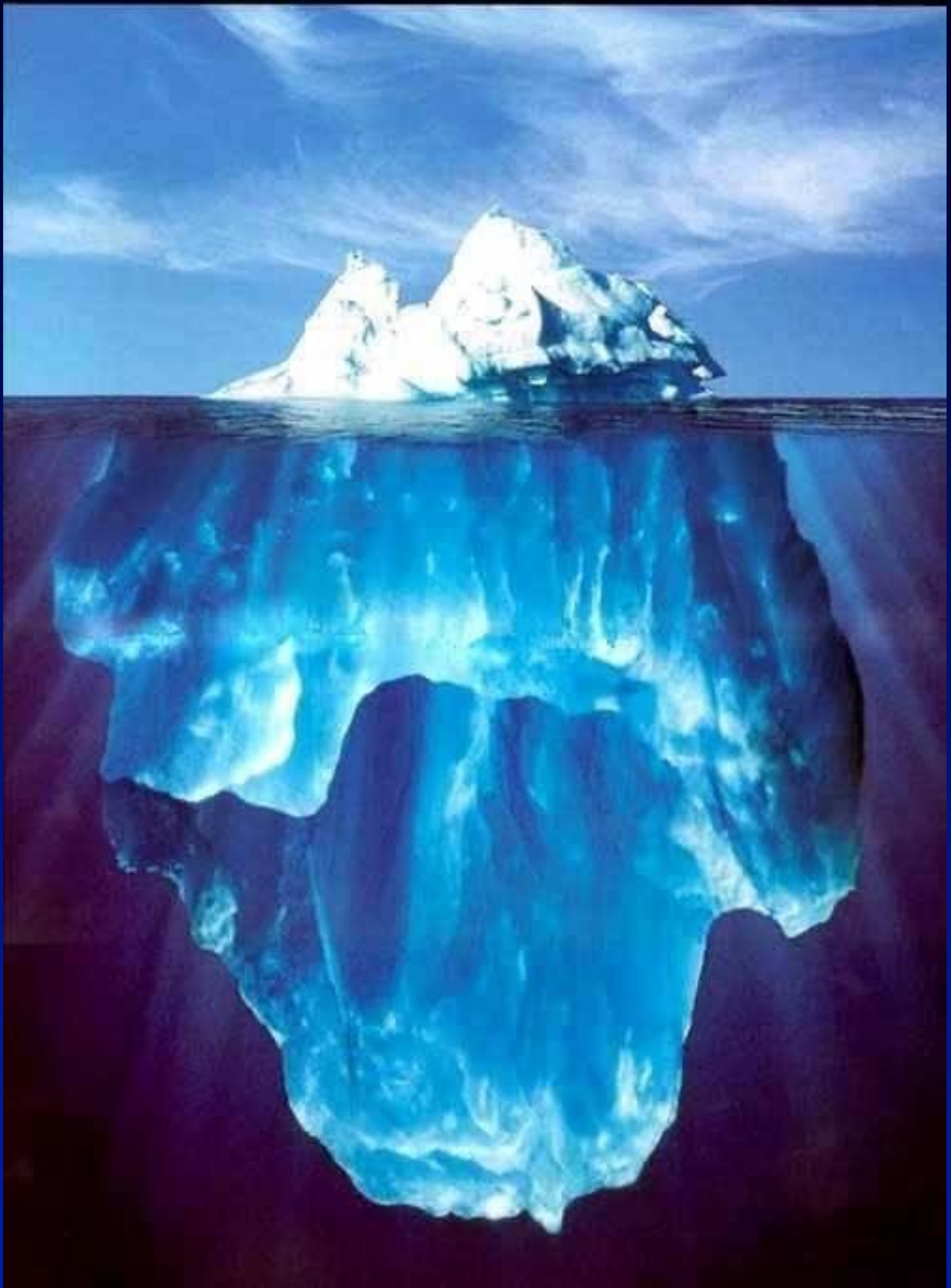

GISMO-2: Funded by NSF

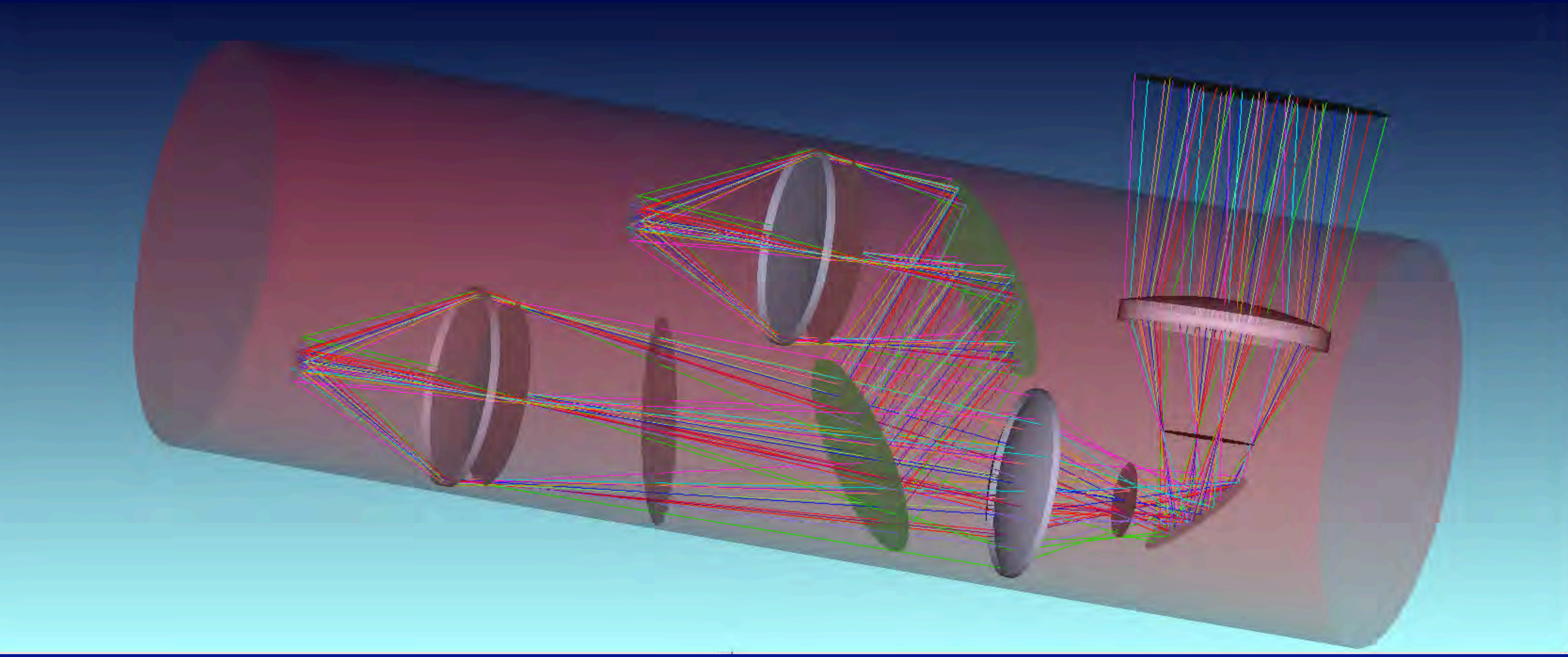

GISMO Picture Gallery

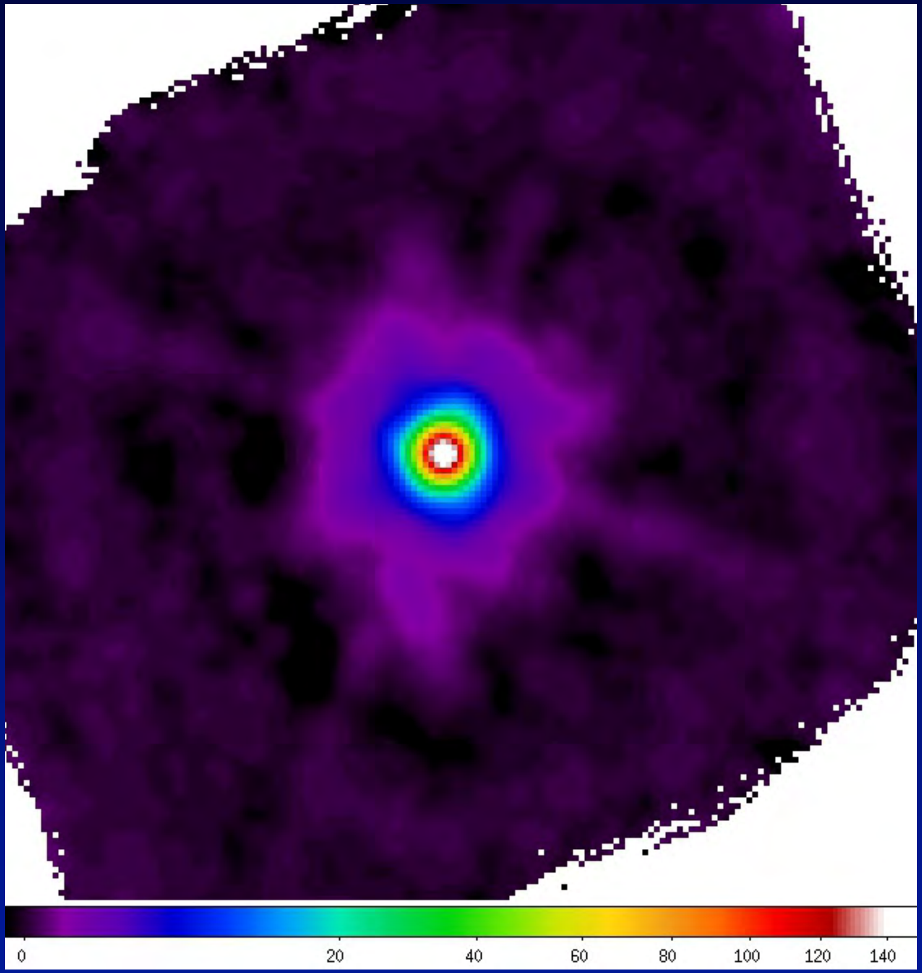

Mars

GISMO Picture Gallery

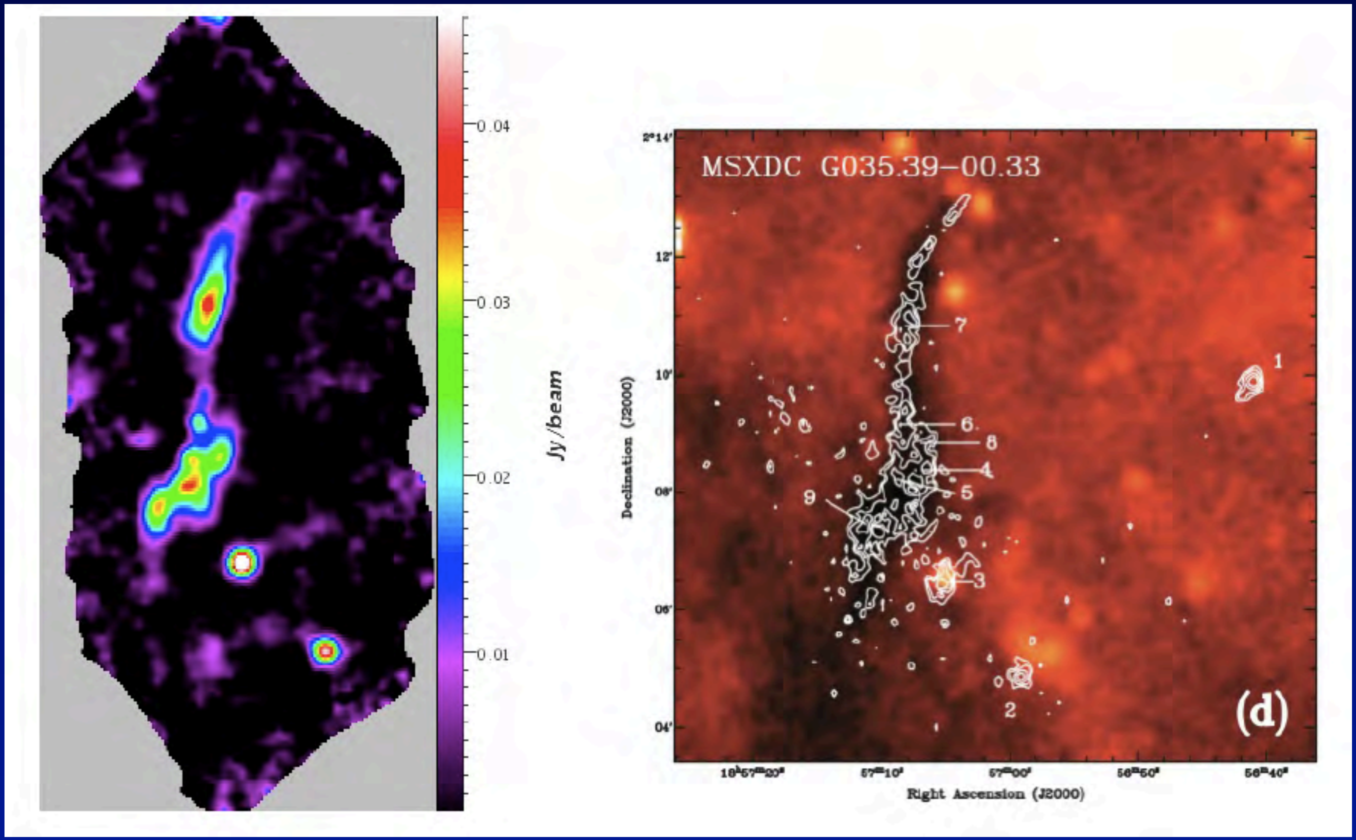

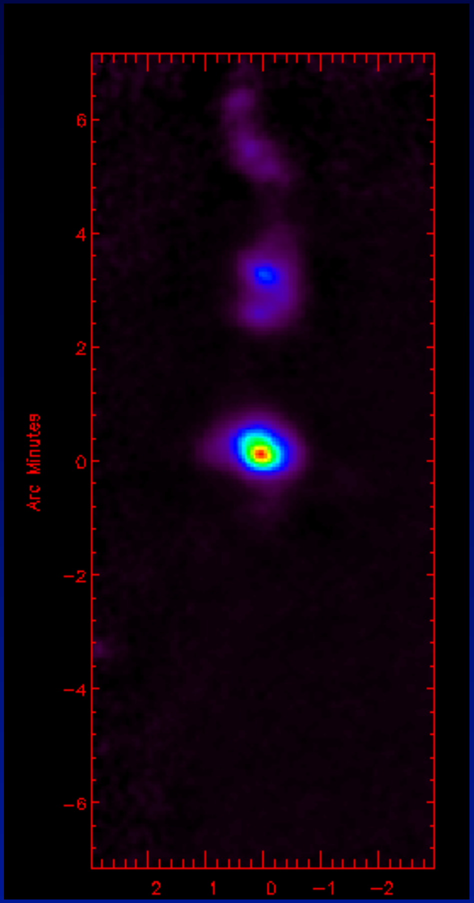

InfraRed Dark Clouds (IRDC)
GISMO (left), MAMBO-2 & IRAC 8 μm (Rathborne et al. 2006)

SF Region
Dr21

GISMO Picture Gallery

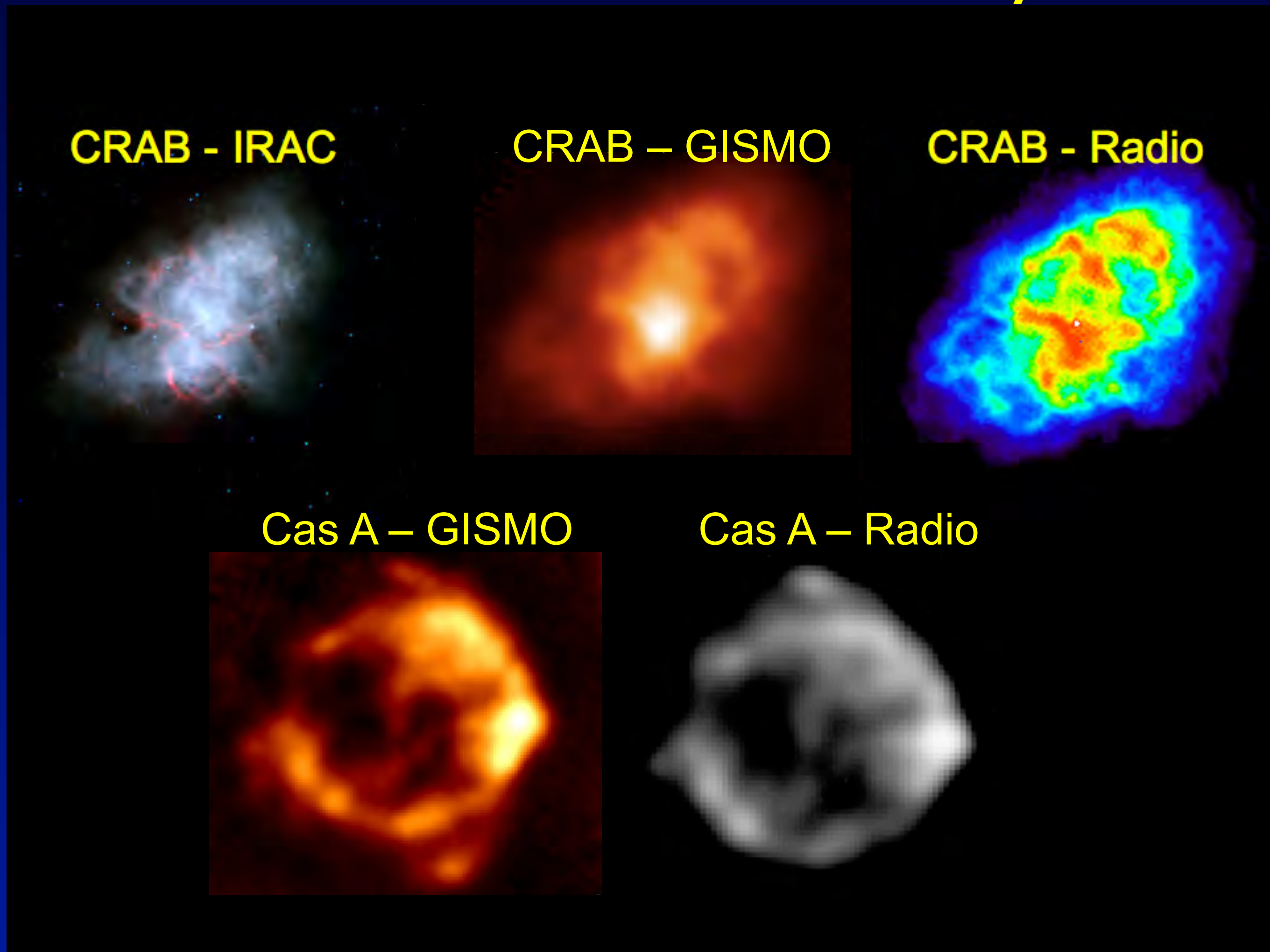

Super Nova Remnants (SNR)

GISMO Picture Gallery

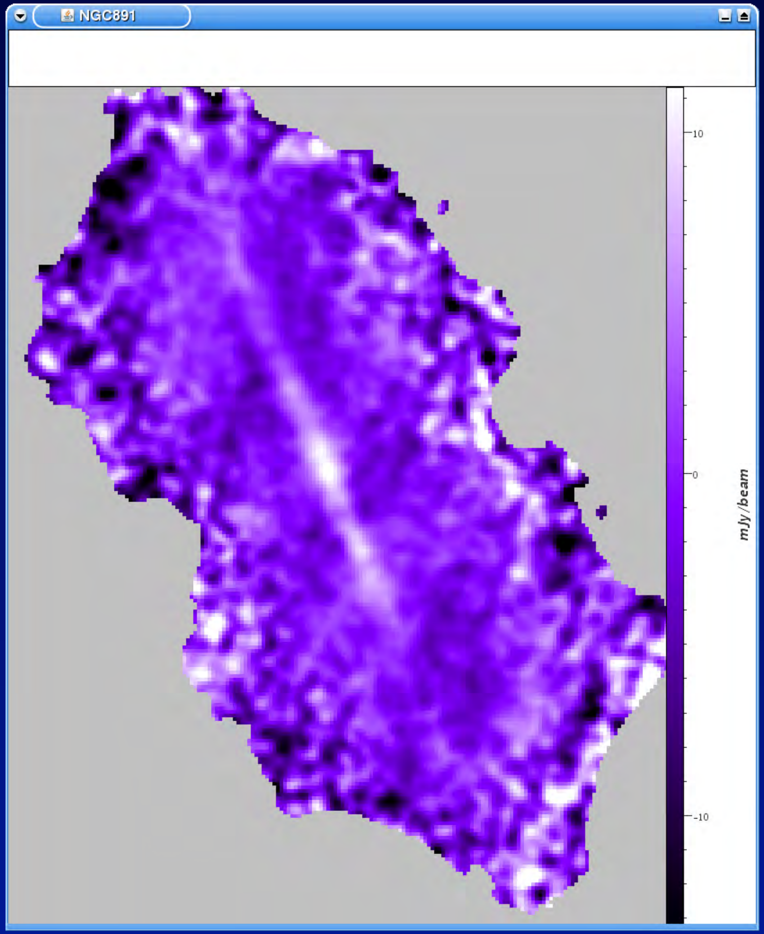

NGC891

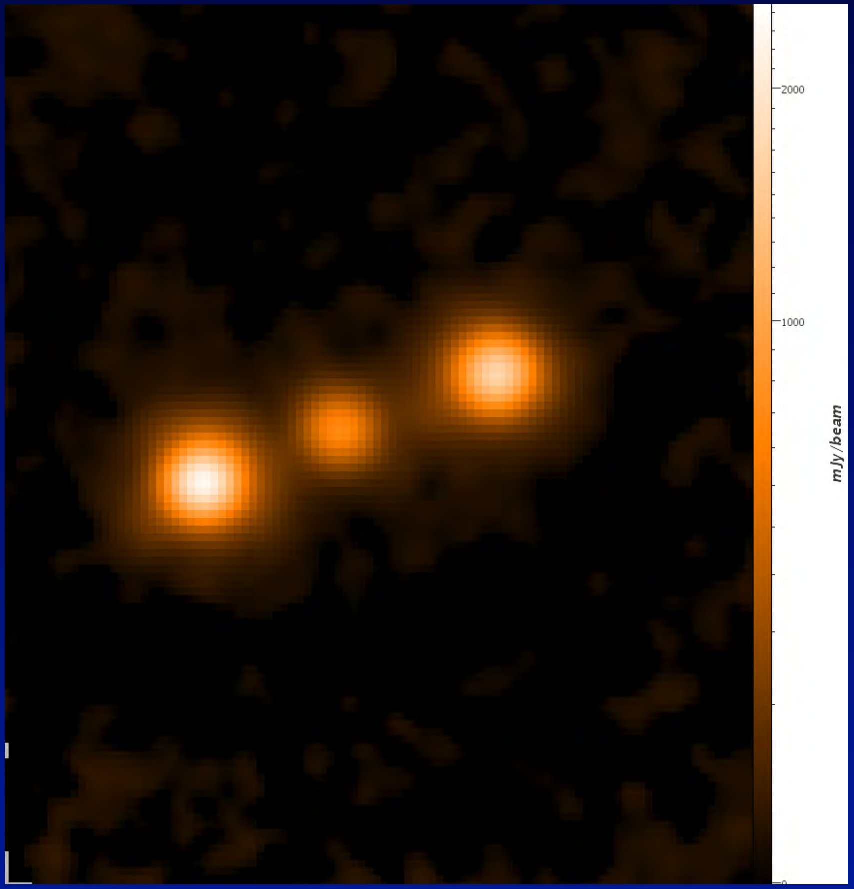

Cyg A

GISMO's Primary Science

- Galaxy evolution: number counts, star- and dust- formation history
- Galaxy formation: feedback, environment in the very high redshift universe
- Clustering of Galaxies
- Complement existing surveys and provide Target Lists for JWST, ALMA
- Cold dust in the local universe
- Free-free emission from starbursts

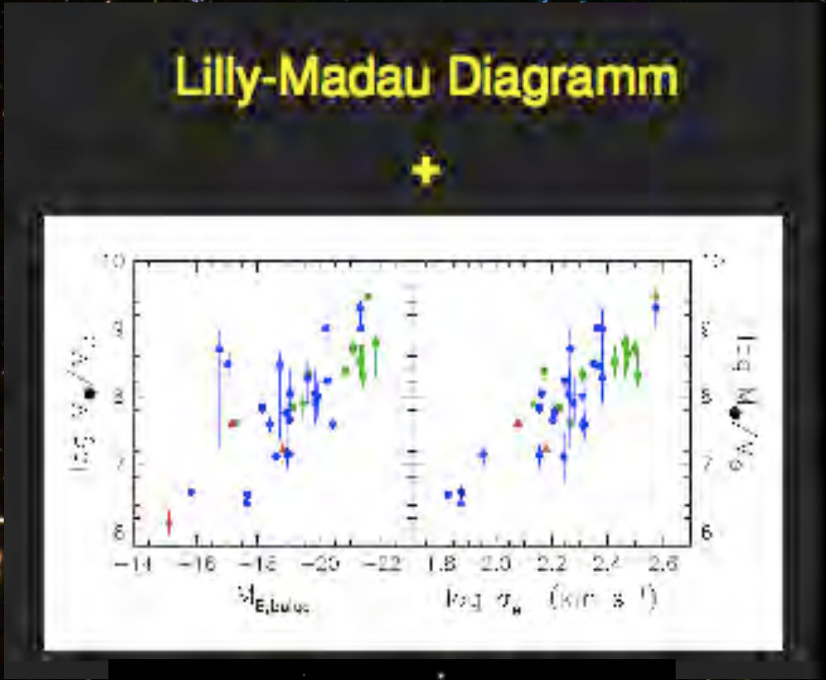

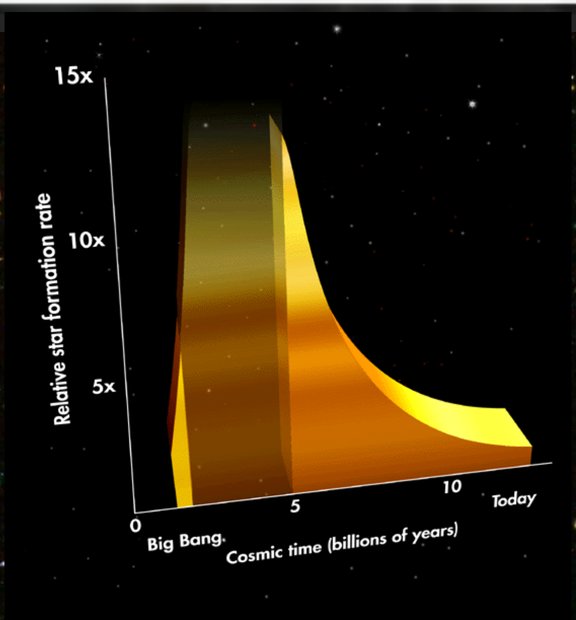

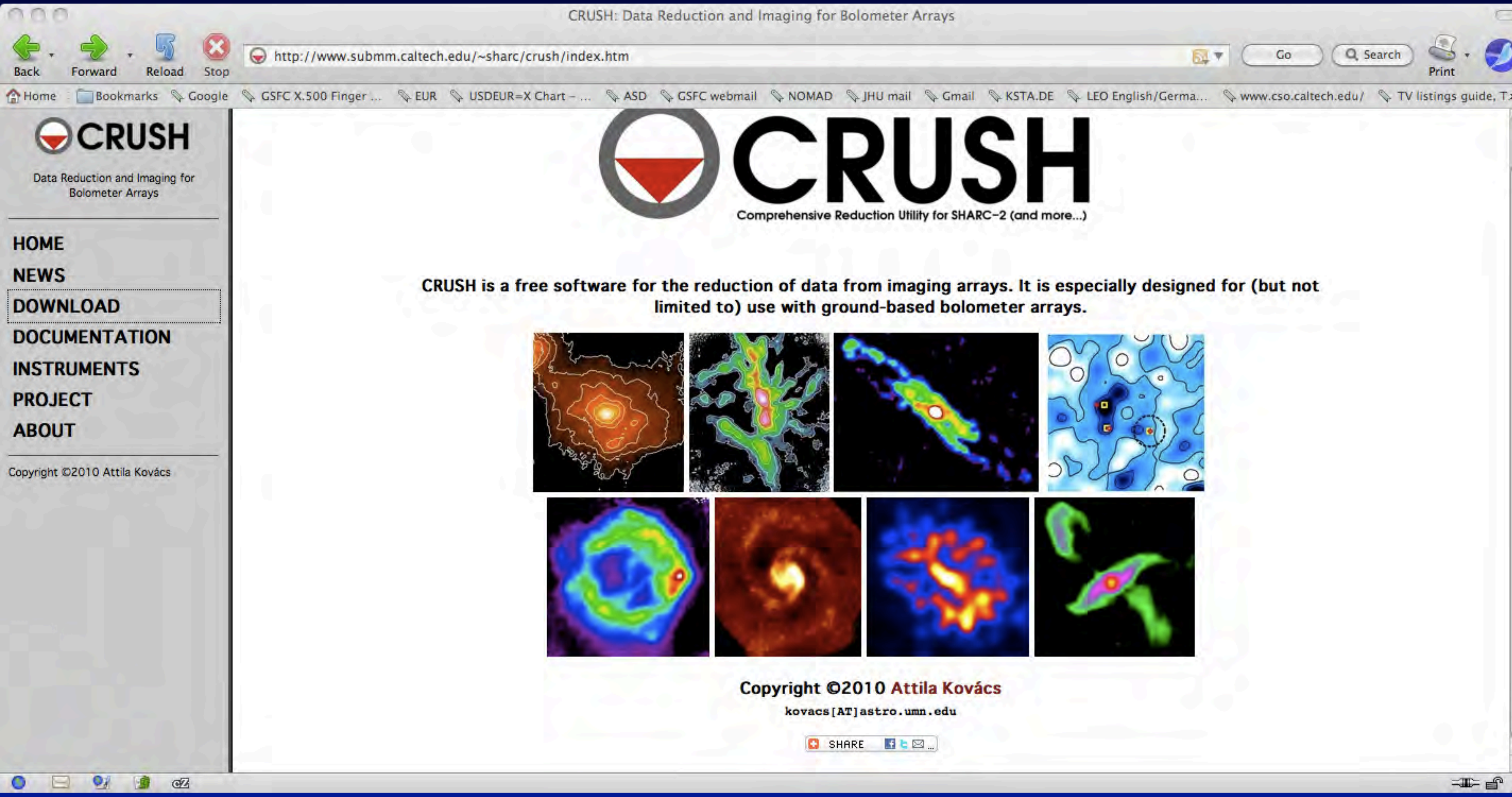
CRUSH: Data Reduction and Imaging for Bolometer Arrays
http://www.submm.caltech.edu/~sharc/crush/index.htm
CRUSH
Data Reduction and Imaging for Bolometer Arrays
HOME
NEWS
DOWNLOAD
DOCUMENTATION
INSTRUMENTS
PROJECT
ABOUT
Copyright ©2010 Attila Kovács
CRUSH
Comprehensive Reduction Utility for SHARC-2 (and more...)
CRUSH is a free software for the reduction of data from imaging arrays. It is especially designed for (but not limited to) use with ground-based bolometer arrays.
Copyright ©2010 Attila Kovács
kovacs[AT]astro.umn.edu
SHARE

GISMO 2mm Camera Science

Mapping Sensitivity

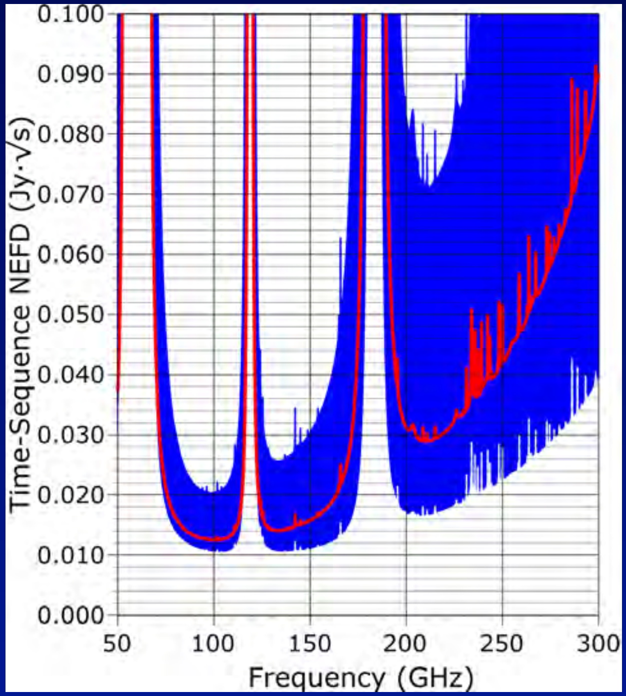

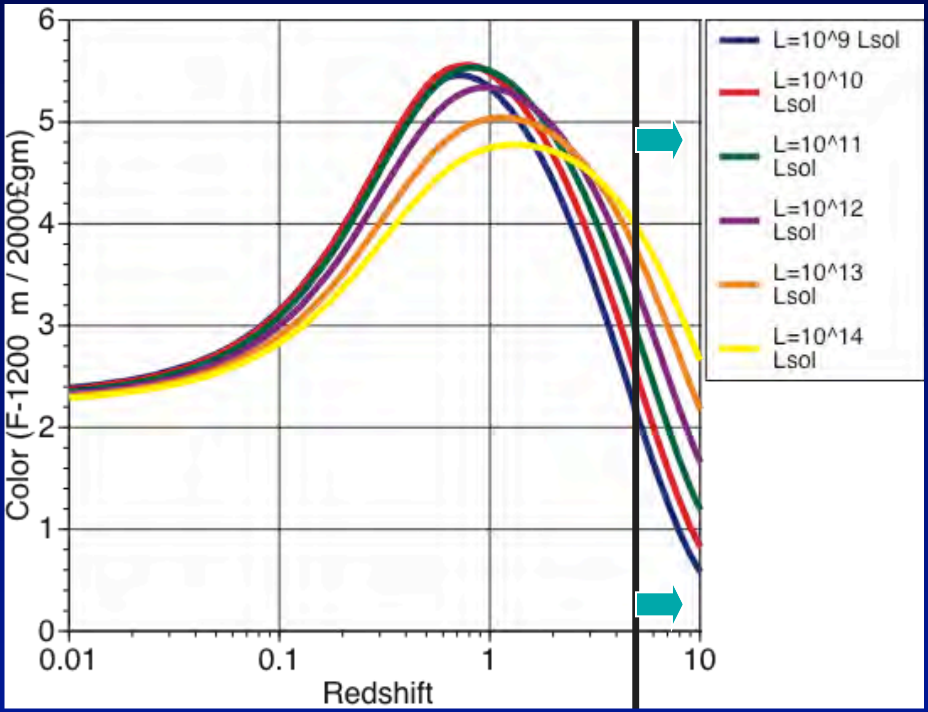

detection speed/pixel of high-z galaxies for $z \geq 5$ is better than at 1.2 mm

GISMO-2

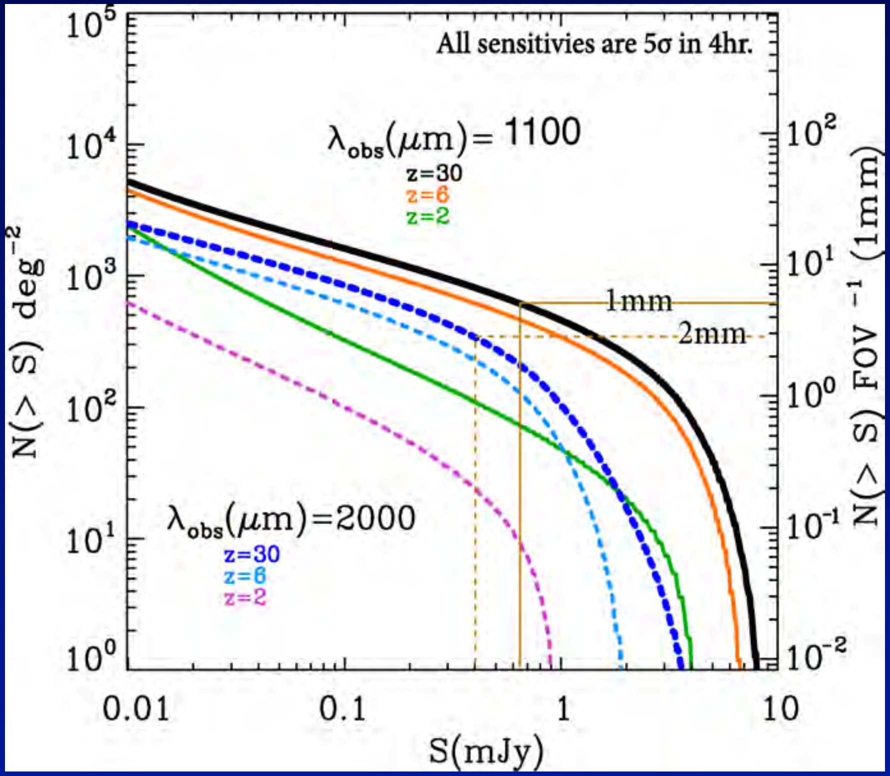

All sensitivies are 5σ in 4hr.
$\lambda_{obs}(\mu m) = 1100$
z=30
z=6
z=2
1mm
2mm
$\lambda_{obs}(\mu m)=2000$
z=30
z=6
z=2
$N(>S)\ deg^{-2}$
$N(>S)\ FOV^{-1}\ (1mm)$
S(mJy)

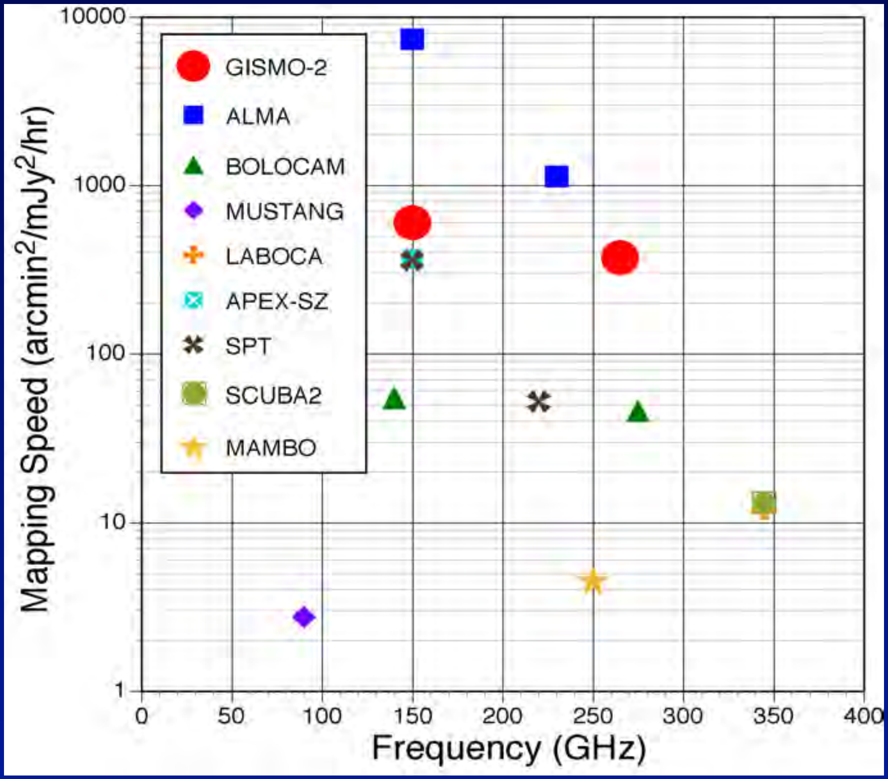

GISMO-2
ALMA
BOLOCAM
MUSTANG
LABOCA
APEX-SZ
SPT
SCUBA2
MAMBO
Mapping Speed (arcmin²/mJy²/hr)
Frequency (GHz)

GISMO – Detector performance

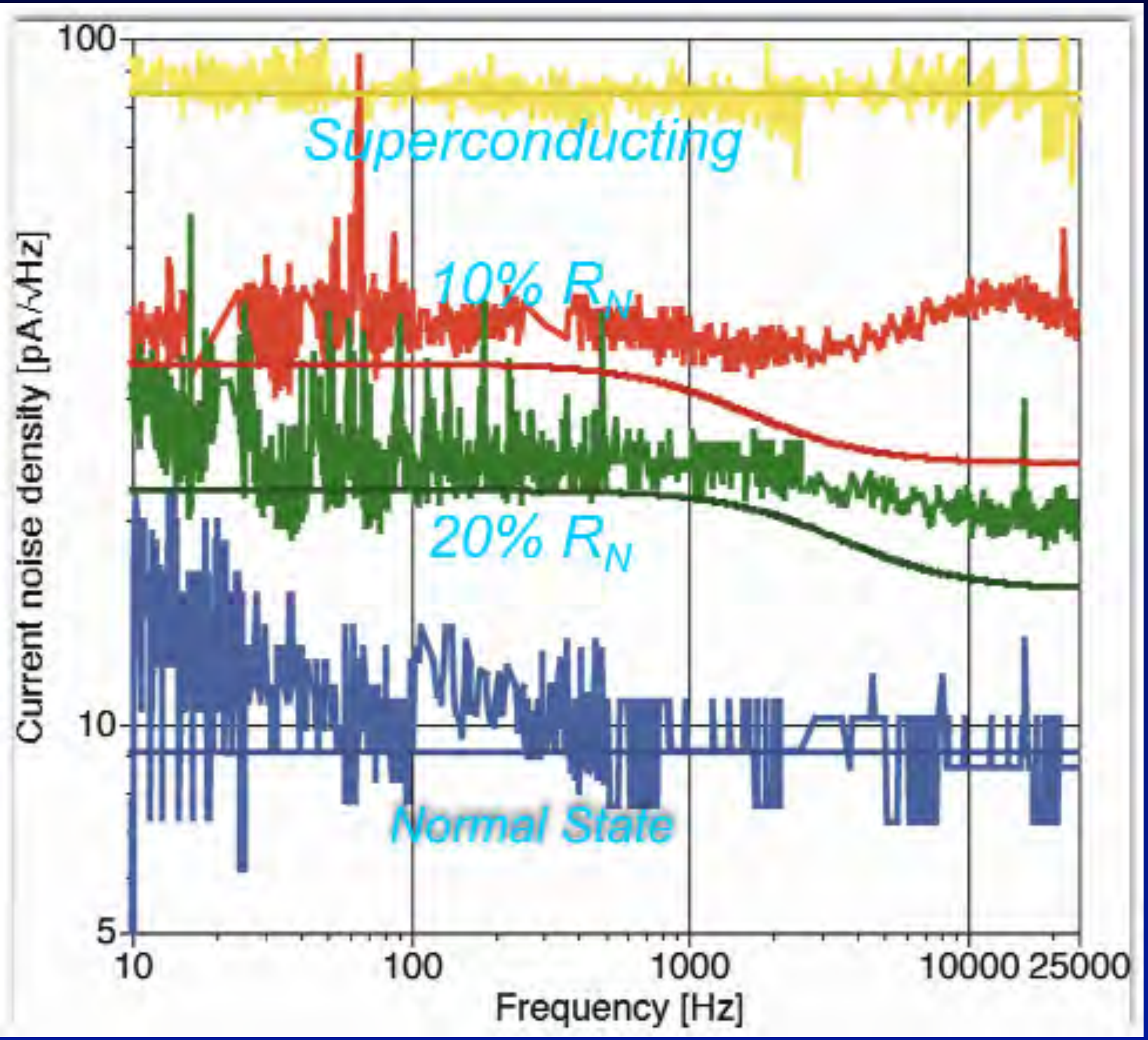

GISMO Eyelash: Evidence for SZ?

Warning: very preliminary!!!!

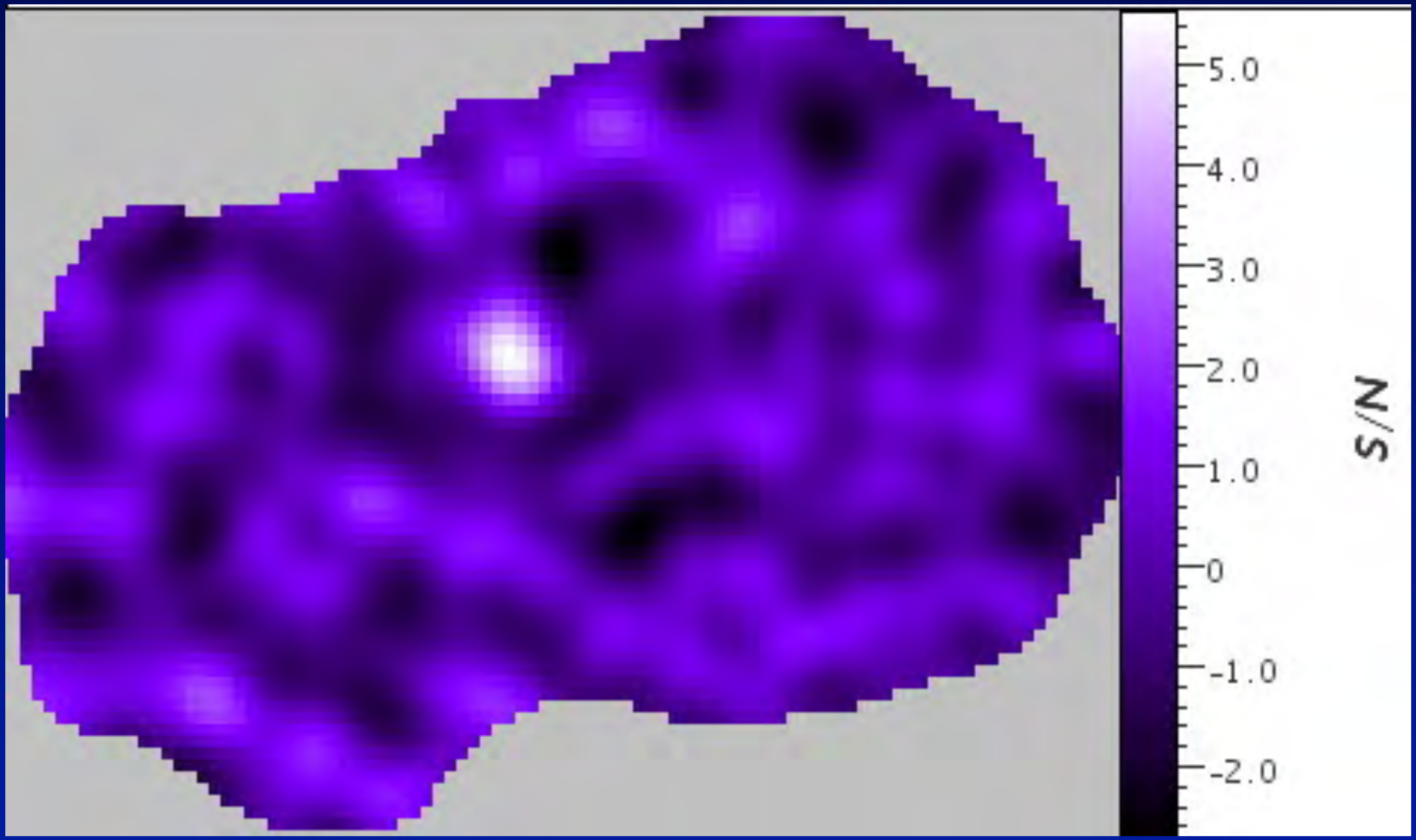

Conclusions

- AzTEC-3 is $z = 5.3$ starburst galaxy with a starburst age of ~ 200 Myr
- Only a Top Heavy IMF fits data
- The dust mass of ≈ $1 \times 10^9\ M_{sun}$ provides crucial constraints on SF history
- SFR ~ 500 $M_\odot\ yr^{-1}$, $M_\odot \sim 3 \times 10^{10}\ M_\odot$
- Most of the galaxy's mass is in the gas phase
- More/deeper (sub-)millimeter wave data are needed to derive a more accurate dust mass

LETTER

doi:10.1038/nature09681

A massive protocluster of galaxies at a redshift of $z \approx 5.3$

Peter L. Capak[1], Dominik Riechers[2], Nick Z. Scoville[2], Chris Carilli[3], Pierre Cox[4], Roberto Neri[4], Brant Robertson[2], Mara Salvato[5], Eva Schinnerer[6], Lin Yan[1], Grant W. Wilson[7], Min Yun[7], Francesca Civano[8], Martin Elvis[8], Alexander Karim[6], Bahram Mobasher[9] & Johannes G. Staguhn[10]

Massive clusters of galaxies have been found that date from as early as 3.9 billion years[1] (3.9 Gyr; $z = 1.62$) after the Big Bang, containing stars that formed at even earlier epochs[2,3]. Cosmological simulations using the current cold dark matter model predict that these systems should descend from 'protoclusters'—early overdensities of massive galaxies that merge hierarchically to form a cluster[4,5]. These protocluster regions themselves are built up hierarchically and so are expected to contain extremely massive galaxies that can be observed as luminous quasars and starbursts[4–6]. Observational evidence for this picture, however, is sparse because high-redshift protoclusters are rare and difficult to observe[6,7]. Here we report a protocluster region that dates from 1 Gyr ($z = 5.3$) after the Big Bang. This cluster of massive galaxies extends over more than 13 megaparsecs and contains a luminous quasar as well as a system rich in molecular gas[8]. These massive galaxies place a lower limit of more than 4×10^{11} solar masses of dark and luminous matter in this region, consistent with that expected from cosmological simulations for the earliest galaxy clusters[4,5,7].

Cosmological simulations predict that the progenitors of present-day galaxy clusters are the largest structures at high redshift[4,5,7] ($M_{\rm halo} > 2 \times 10^{11}$ solar masses ($M_\odot$) and $M_{\rm stars} > 4 \times 10^9 M_\odot$ at $z \approx 6$). These protocluster regions should be characterized by local overdensities of massive galaxies on co-moving distance scales of 2–8 Mpc that coherently extend over tens of megaparsecs, forming a structure that will eventually coalesce into a cluster[4,5,7,9]. Furthermore, owing to the high mass densities and correspondingly high merger rates, extreme phenomena such as starbursts and quasars should preferentially exist in these regions[4–7,9,10]. Although overdensities have been reported around radio galaxies on ~10–20-Mpc scales[6,7] and large gas masses around quasars[11,12] at redshifts greater than $z = 5$, the available data is not comprehensive enough to constrain the mass of these protoclusters and hence provide robust constraints on cosmological models[6,7,9].

We used data covering the entire accessible electromagnetic spectrum in the 2-square-degree Cosmological Evolution Survey (COSMOS) field[13] (right ascension, 10 h 00 min 30 s; declination, 2° 30′ 00″) to search for starbursts, quasars and massive galaxies as signposts of potential overdensities at high redshift. This deep, large-area field provides the multiwavelength data required to find protoclusters on scales >10 Mpc (5′). Optically bright objects at redshifts greater than $z = 4$ were identified through optical and near-infrared colours. Extreme star formation activity was found using millimetre-wave[14,15] and radio[16] measurements, and potential luminous quasars were identified by X-ray measurements[17]. Finally, extreme objects and their surrounding galaxies were targeted with the Keck II telescope and the Deep Extragalactic Imaging Multi-Object Spectrograph (W. M. Keck Observatory, Hawaii) to measure redshifts.

We found a grouping of four major objects at $z = 5.30$ (Fig. 1). The most significant overdensity appears near the extreme starburst galaxy COSMOS AzTEC-3, which contains $>5.3 \times 10^{10} M_\odot$ of molecular gas and has a dynamical mass, including dark matter, of $>1.4 \times 10^{11} M_\odot$ (ref. 8). The far-infrared (60–120-μm) luminosity of this system is estimated to be $(1.7 \pm 0.8) \times 10^{13}$ solar luminosities ($L_\odot$), corresponding to a star formation rate of $>1{,}500 M_\odot$ per year[18], which is >100 times the rate of an average galaxy (with luminosity L_*) at $z = 5.3$ (ref. 19). The value and error given are the mean estimate and scatter derived from empirical estimates based on the sub-millimetre flux, radio flux limit, and CO luminosity, along with model fitting. The models predict a much broader range in total infrared (8–1,000-μm) luminosities, ranging from $2.2 \times 10^{13} L_\odot$ to $11 \times 10^{13} L_\odot$. The large uncertainty results from the many assumptions used in the models, combined with a lack of data constraining the infrared emission at wavelengths less than rest-frame 140 μm. However, the

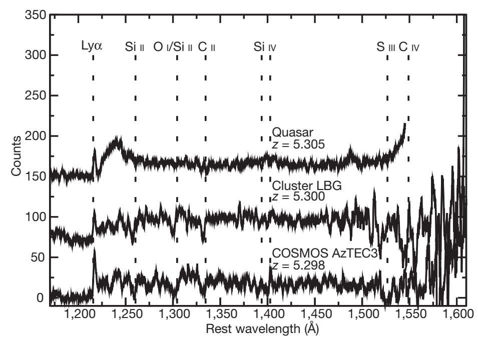

Figure 1 | Spectra of confirmed cluster members. These spectra were taken with the Keck II telescope and correspond to the extreme starburst (COSMOS AzTEC3), a combined spectrum of two Lyman-break galaxies at 95 kpc (Cluster LBG) and the Chandra-detected quasar at 13 Mpc from the extreme starburst. The galaxy spectra show absorption features indicative of interstellar gas (Si II, O I/Si II and C II) and young massive stars (Si IV and C IV) indicative of a stellar population less than 30 Myr old[26]. The quasar shows broad Lyman-α (Lyα) emission absorbed by strong winds, with a narrow Lyman-α line seen at the same systemic velocity as absorption features in the spectra.

[1]Spitzer Science Centre, 314-6 California Institute of Technology, 1200 East California Boulevard, Pasadena, California 91125, USA. [2]Department of Astronomy, 249-17 California Institute of Technology, 1200 East California Boulevard, Pasadena, California 91125, USA. [3]National Radio Astronomy Observatory, PO Box O, Socorro, New Mexico 87801, USA. [4]Institut de Radio Astronomie Millimétrique, 300 rue de la Piscine, F-38406 St-Martin-d'Hères, France. [5]Max-Planck-Institute für Plasma Physics, Boltzmann Strasse 2, Garching 85748, Germany. [6]Max-Planck-Institute für Astronomie, Königstuhl 17, Heidelberg 69117, Germany. [7]Department of Astronomy, University of Massachusetts, Lederle Graduate Research Tower B, 619E, 710 North Pleasant Street, Amherst, Massachusetts 01003-9305, USA. [8]Harvard Smithsonian Center for Astrophysics, 60 Garden Street, MS, 67, Cambridge, Massachusetts 02138, USA. [9]Department of Physics and Astronomy, University of California, Riverside, California 92521, USA. [10]Johns Hopkins University, Laboratory for Observational Cosmology, Code 665, Building 34, NASA's Goddard Space Flight Center, Greenbelt, Maryland 20771, USA.

Motivation

Massive clusters of galaxies have been found that date from as early as 4 billion years (z ~1.5) after the Big Bang, containing stars that formed at even earlier epochs

Papovich, C. et al. "A Spitzer-selected galaxy cluster at z~1.62", ApJ, 716, (2010); Mei,S. et al. "Evolution of the color-magnitud relation in galaxy clusters at z=1from the ACS Intermediate Redshift Cluster Survey." ApJ, 690, 42(2009).

CDM models predict that these systems should descend from 'protoclusters'—early overdensities of massive galaxies that merge hierarchically to form a cluster

Springel, V. et al. Simulations of the formation, evolution and clustering of galaxies and quasars. Nature 435, 629–636 (2005).
Li, Y. et al. "Formation of z,6 quasars from hierarchical galaxy mergers" ApJ, 665 (2007).

These protocluster regions themselves are built up hierarchically and so are expected to contain extremely massive galaxies that can be observed as luminous quasars and starbursts.

The Cosmic Evolution Survey (COSMOS)

Area Coverage: 2 square degrees
Wavelength: X-ray to Radio
Lifetime: 2004 – present

Instruments:
* HST (ACS, WFPC2 and NICMOS)
  * Spitzer (IRAC and MIPS)
  * Chandra (ACIS)
  * XMM-Newton (EPIC)
  * Subaru (SuprimeCam)
  * VLA
  * ESO/VLT (VIMOS)
  * Additional ground- and space-based instruments

Science Products Generated: Targeted deep survey using wide range of ground and space image data, catalogs, and spectra.

GISMO 2mm Camera Science

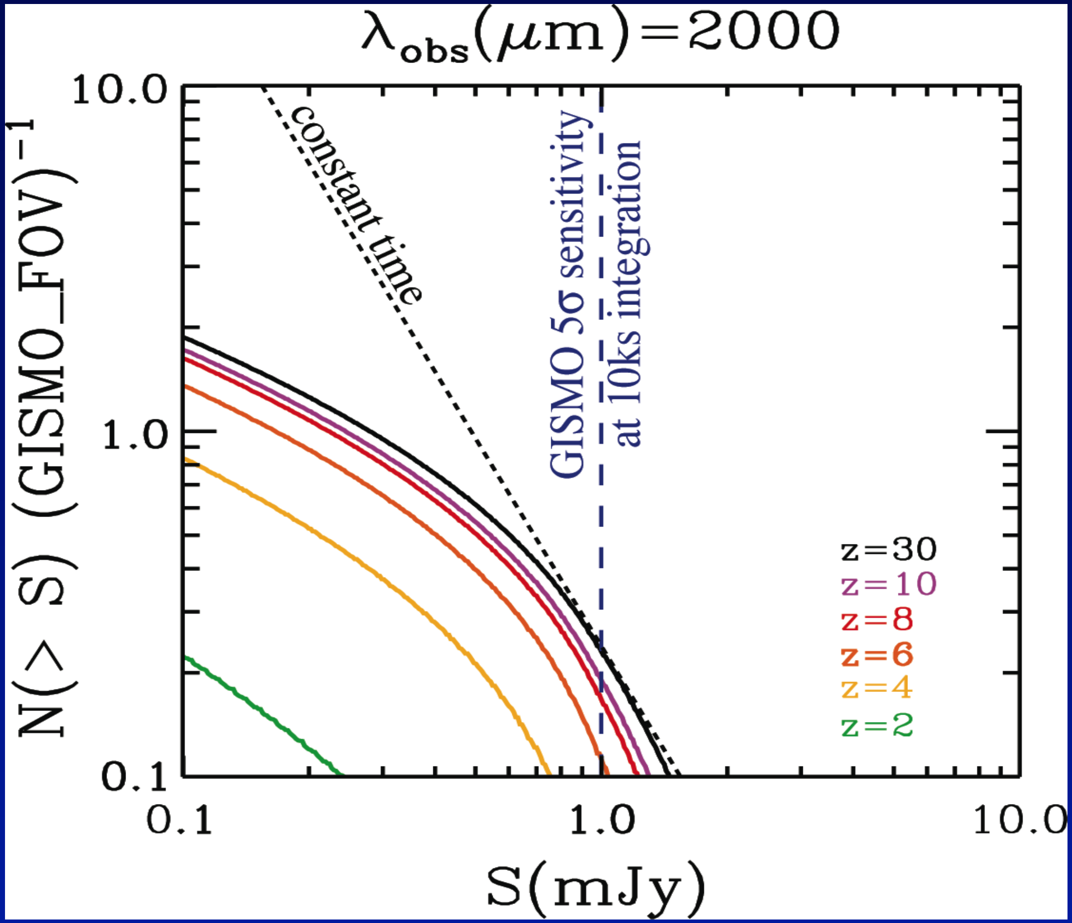

N(>S) @ 2 mm for GISMO instantaneous sky coverage versus flux

SED of Starburst Galaxy Arp 220 for different redshifts
MAMBO 1200 μm

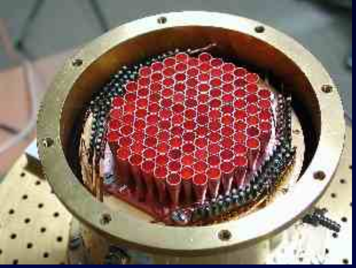

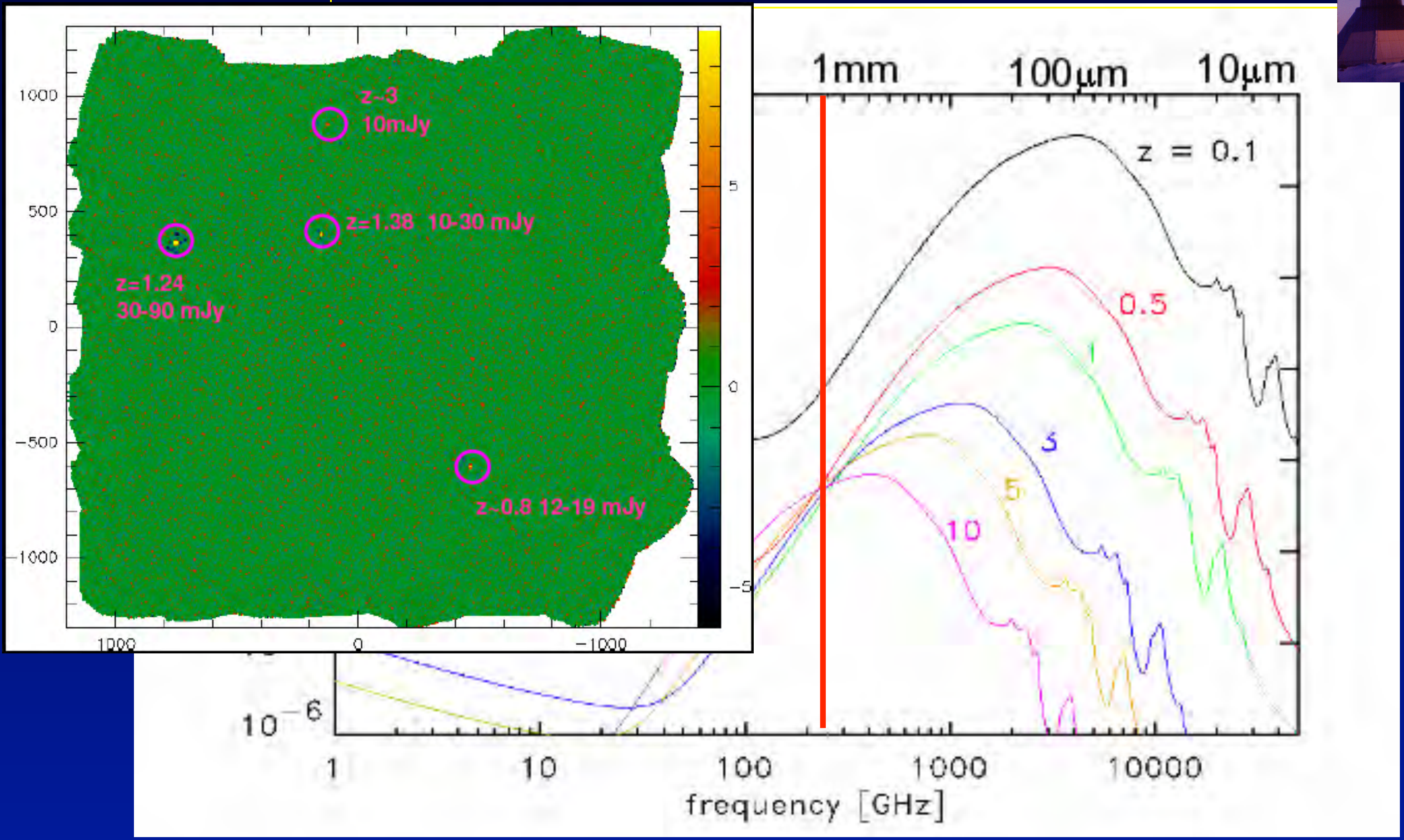

Goddard Space Flight Center

GISMO 2mm Camera Science

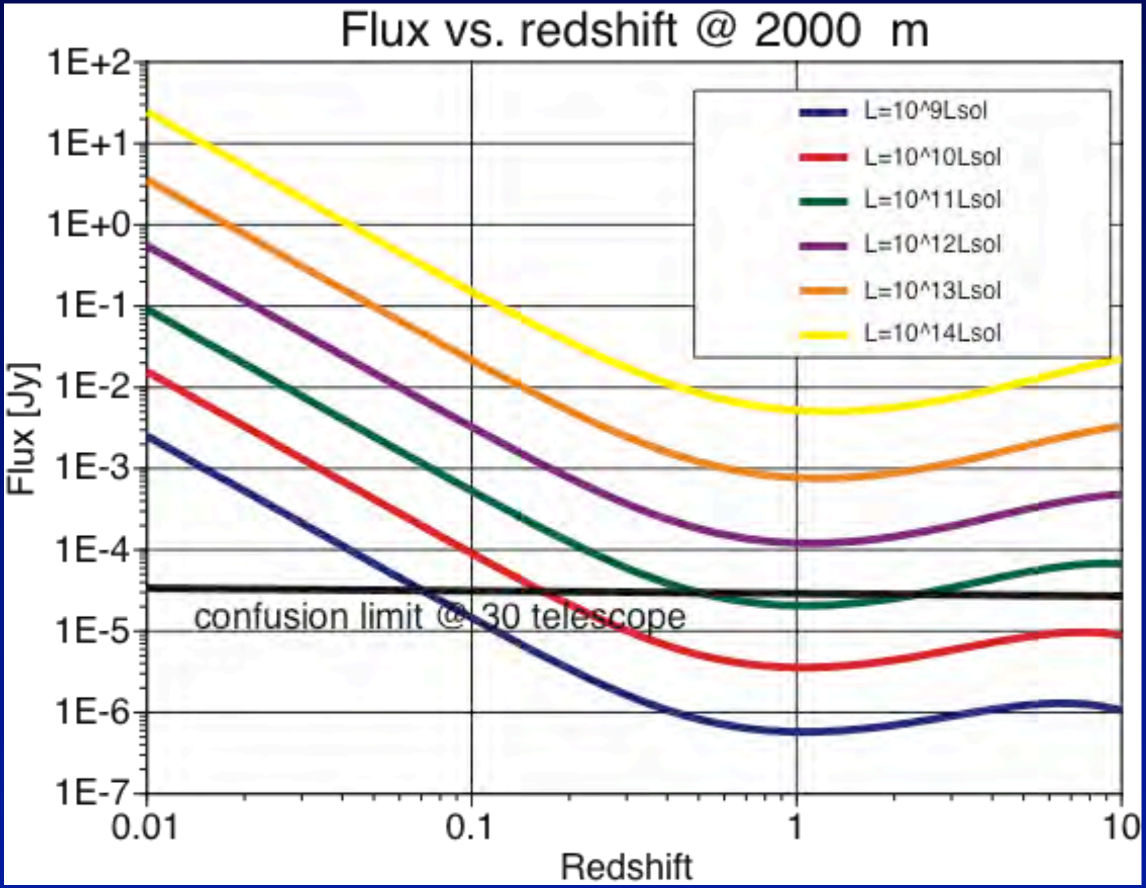

Beating the Confusion Limit

30 m Telescope:

: 1.2 mm

: 2 mm

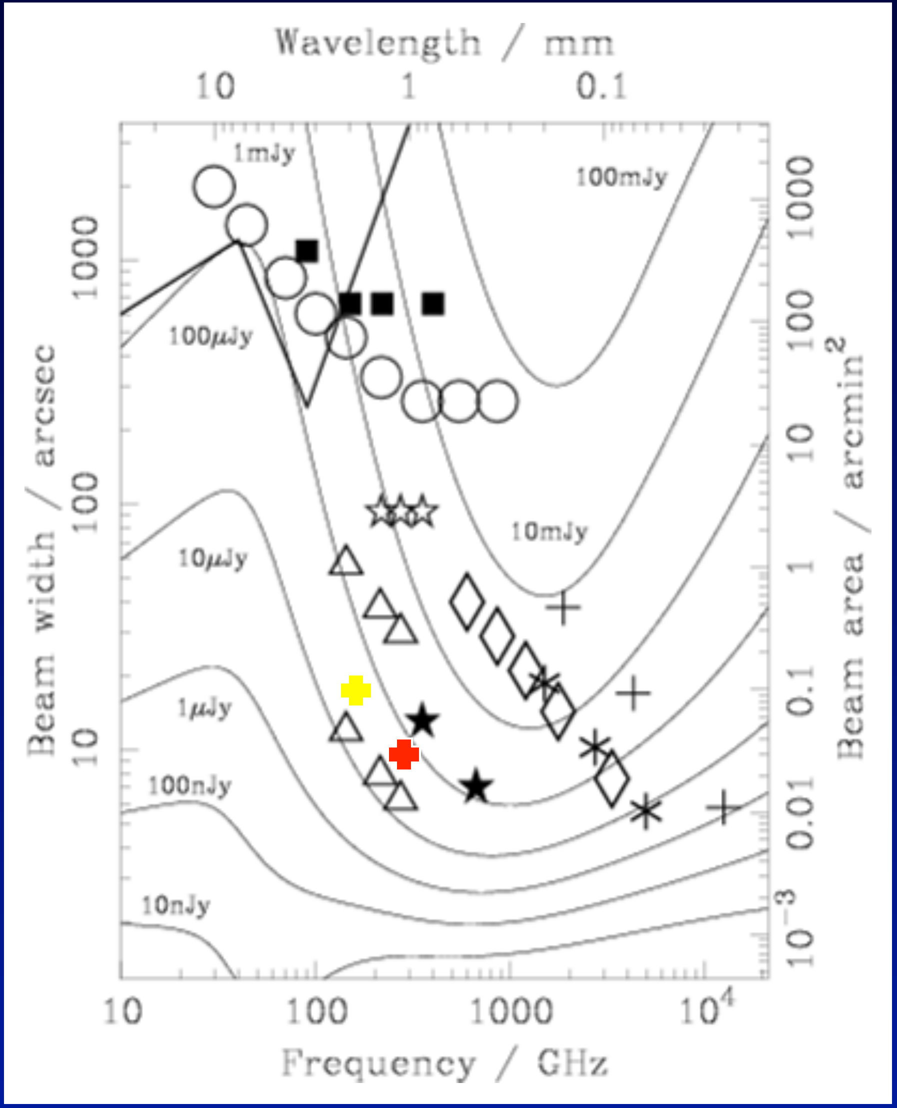

Plot: A. Blain

GISMO 2mm Camera Science

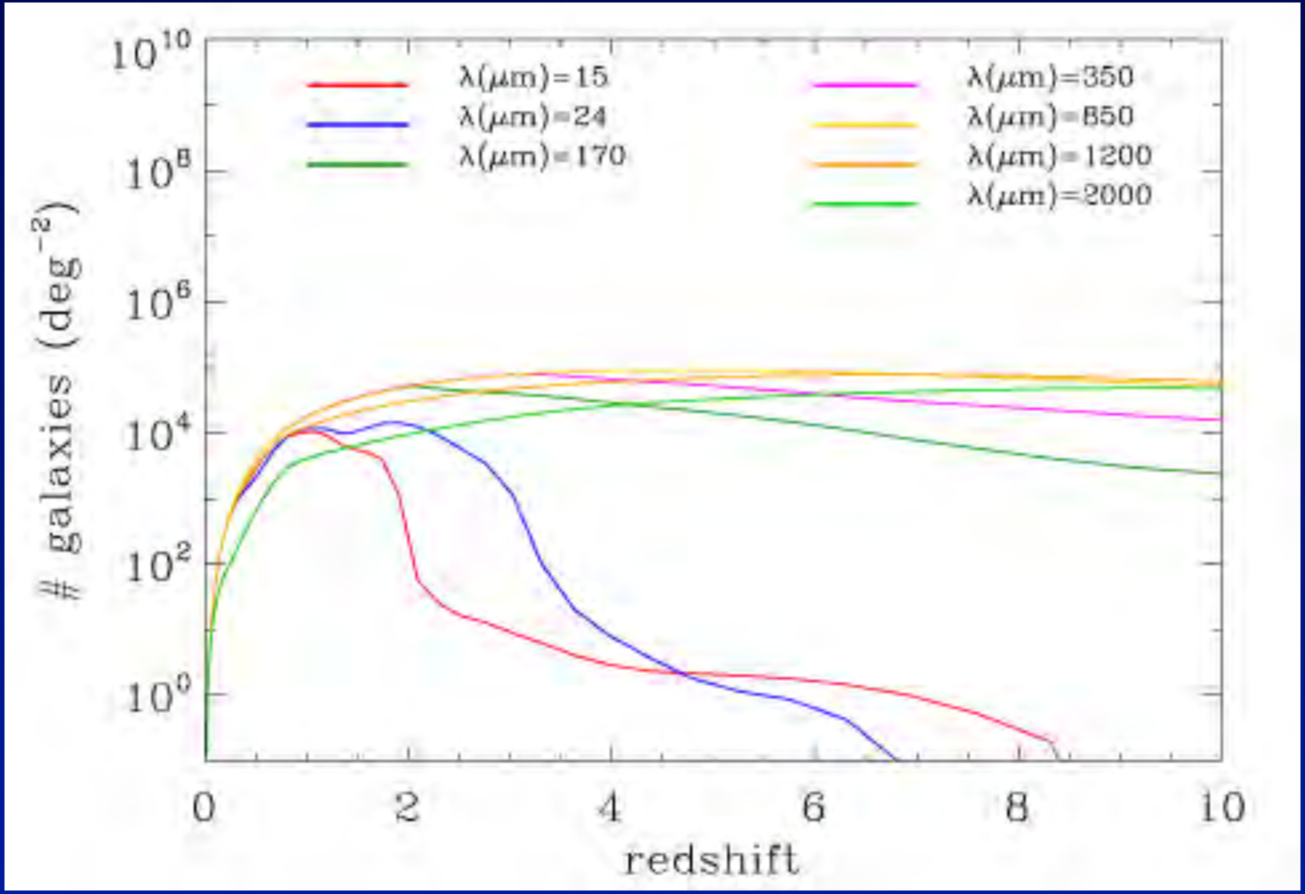

GISMO-2

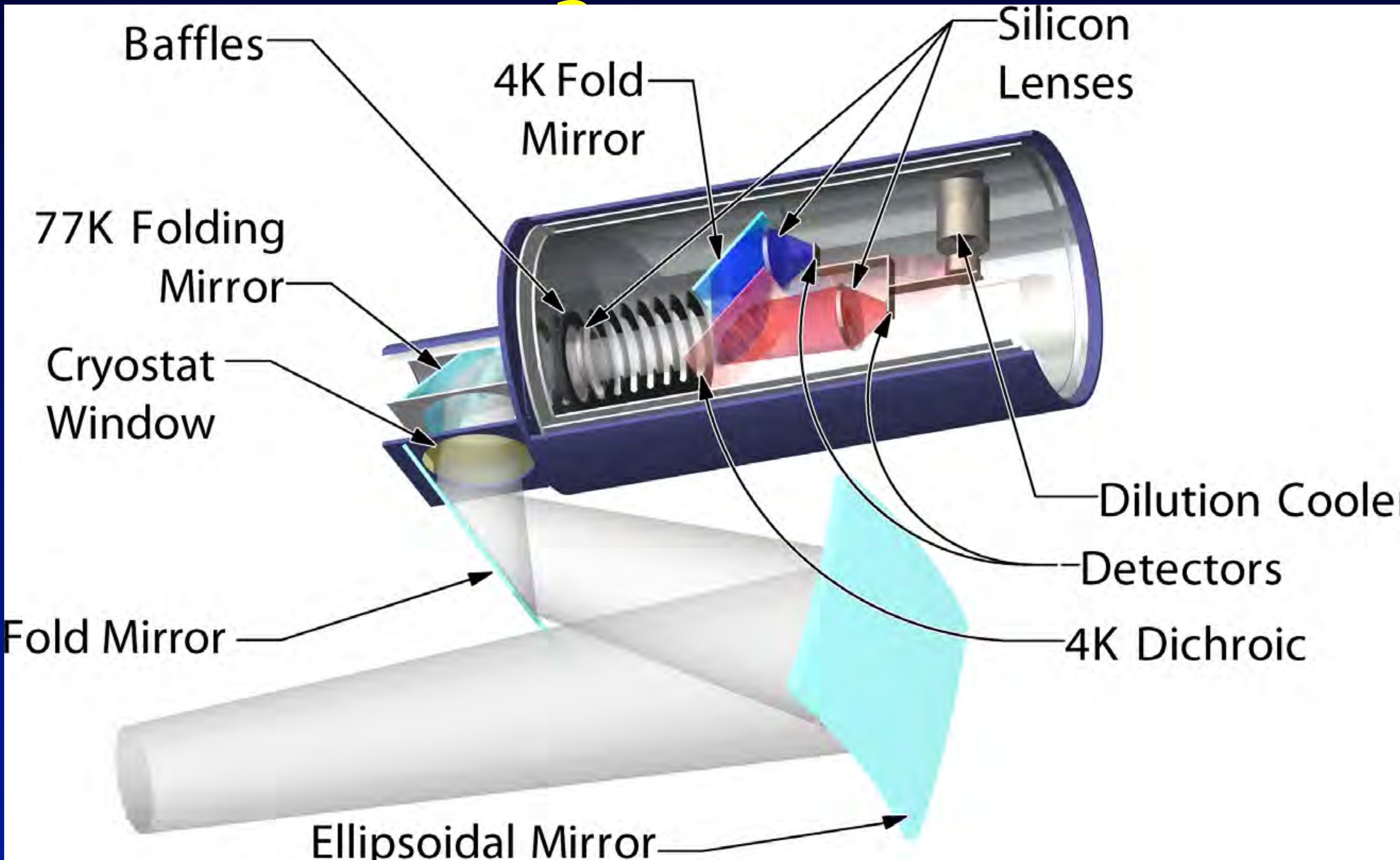

jstaguhn@pha.jhu.edu or johannes.staguhn@nasa.gov

GISMO Deep Field

rms in innermost 5’ (shown): 120 μJy (until now Deepest Field SCUBA: ~ 400 μJy)

t_{int} = 25 hrs calibration uncertainty: 7%

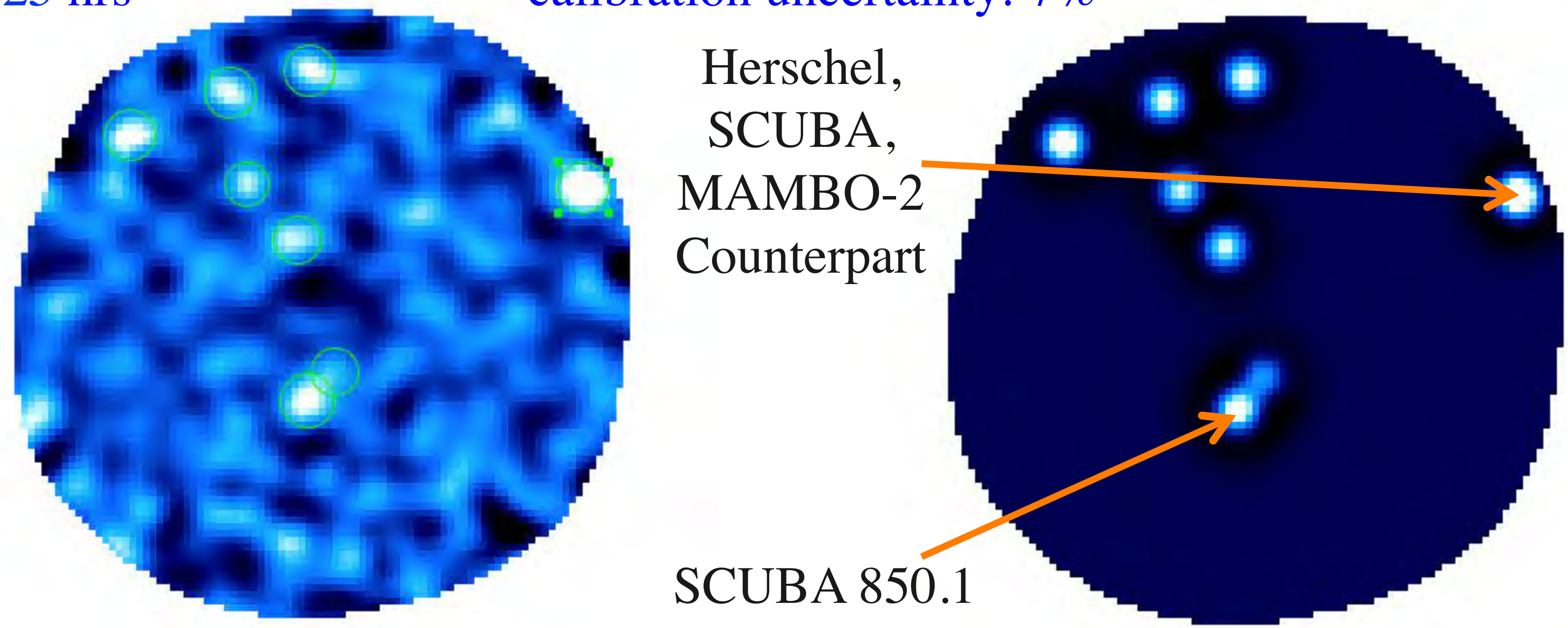

measured flux of detected sources between ~340 μJy and 600 μJy

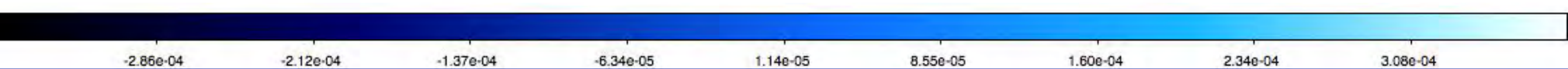

SCUBA Deep Field

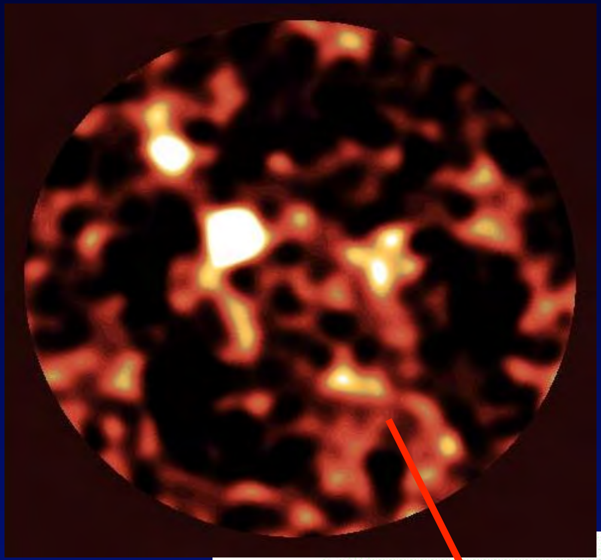

Hughes, 1998

Hubble Deep Field